

AD-A129 154

REACTIONS OF METAL-METAL MULTIPLE BONDS. 10 REACTIONS OF
MO₂(OR)₆ (M TRIPL.) (U) INDIANA UNIV AT BLOOMINGTON DEPT
OF CHEMISTRY M H CHISHOLM ET AL. 06 JUN 83

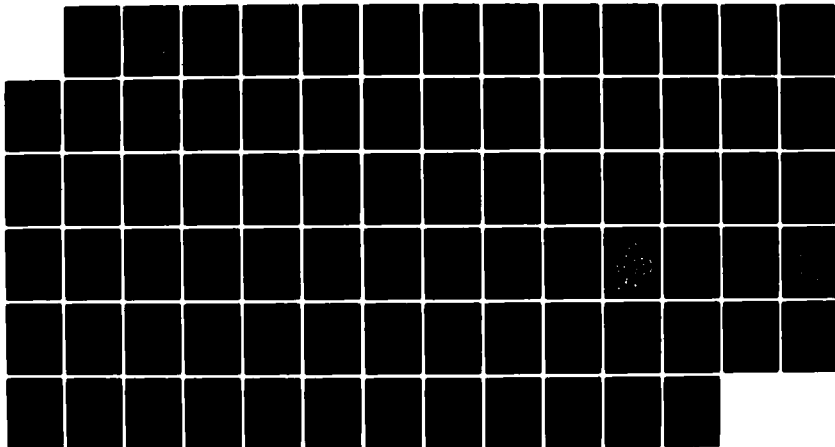
1/1

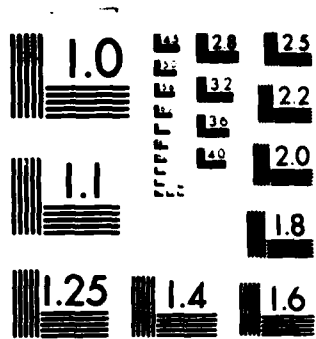
UNCLASSIFIED

INDU/DC/TR-83/2-MC N00014-79-C-0044

F/G 7/2

NL





MICROCOPY RESOLUTION TEST CHART
NATIONAL BUREAU OF STANDARDS-1963-A

AD A 1 291 54

6

OFFICE OF NAVAL RESEARCH

Contract No. N00014-79-C-0044

Task No. NR 056-703

TECHNICAL REPORT NO. INDU/DC/TR-83/2-MC

REACTIONS OF METAL-METAL MULTIPLE BONDS. 10.

REACTIONS OF $\text{Mo}_2(\text{OR})_6$ ($\text{M}=\text{M}$) and $[\text{M}(\text{OR})_4]_x$ COMPOUNDS WITH
MOLECULAR OXYGEN. PREPARATION AND CHARACTERIZATION OF OXO-ALKOXIDES OF
FORMULA $\text{MoO}_2(\text{OR})_2$, $\text{MoO}_2(\text{OR})_2(\text{bpy})$, $\text{MoO}(\text{OR})_4$, $\text{Mo}_3\text{O}(\text{OR})_{10}$,
 $\text{Mo}_4\text{O}_8(\text{OR})_4(\text{py})_4$ AND $\text{Mo}_6\text{O}_{10}(\text{OR})_{12}$.

by

M.H. Chisholm, K. Foltg, J.C. Huffman and C.C. Kirkpatrick

Prepared for Publication

in

Inorganic Chemistry

Department of Chemistry
Indiana University
Bloomington, IN 47405

June 6, 1983

DTIC
SELECTED
JUN 10 1983
A

DTIC FILE COPY

Reproduction in whole or in part is permitted for
any purpose of the United States Government.

This document has been approved for public release
and sale; its distribution is unlimited.

83 06 10 048

REPORT DOCUMENTATION PAGE		READ INSTRUCTIONS BEFORE COMPLETING FORM
1. REPORT NUMBER INDU/DC/TR-83/2-MC	2. GOVT ACCESSION NO. AD A129154	3. RECIPIENT'S CATALOG NUMBER
4. TITLE (and Subtitle) Reactions of Metal-Metal Multiple Bonds. 10. Reactions of $\text{Mo}_2(\text{OR})_6$ (MEM) and $[\text{M}(\text{OR})_4]_x$ Compounds with Molecular Oxygen. Preparation and Characterization of Oxo-Alkoxides of Molybdenum of Formula ...		5. TYPE OF REPORT & PERIOD COVERED Technical Report 1983
7. AUTHOR(s) M.H. Chisholm, K. Folting, J.C.. Huffman and C.C. Kirkpatrick		6. PERFORMING ORG. REPORT NUMBER INDU/DC/TR-83/2-MC
9. PERFORMING ORGANIZATION NAME AND ADDRESS Department of Chemistry Indiana University Bloomington, IN 47405		8. CONTRACT OR GRANT NUMBER(s) N00014-79-C-0044
11. CONTROLLING OFFICE NAME AND ADDRESS Office of Naval Research Department of the Navy Arlington, VA 22217		10. PROGRAM ELEMENT, PROJECT, TASK AREA & WORK UNIT NUMBERS
14. MONITORING AGENCY NAME & ADDRESS (if different from Controlling Office)		12. REPORT DATE June 6, 1983
		13. NUMBER OF PAGES 80
		15. SECURITY CLASS. (of this report)
		15a. DECLASSIFICATION/DOWNGRADING SCHEDULE
16. DISTRIBUTION STATEMENT (of this Report) This document has been approved for public release and sale; its distribution is unlimited.		
17. DISTRIBUTION STATEMENT (of the abstract entered in Block 20, if different from Report)		
18. SUPPLEMENTARY NOTES		
19. KEY WORDS (Continue on reverse side if necessary and identify by block number) metal-metal bonds, molecular oxygen, alkoxides, oxo, oxidation, metal clusters, ^{17}O NMR		
20. ABSTRACT (Continue on reverse side if necessary and identify by block number) $\text{Mo}_2(\text{OR})_6$ (MEM) compounds and molecular oxygen react in hydrocarbon solvents to give $\text{MoO}_2(\text{OR})_2$ compounds and alkoxy radicals. For R = t-Bu, the reactions is rapid with no isolable intermediates; for R = i-Pr and CH_2 -t-Bu, intermediates of formula $\text{Mo}_3\text{O}(\text{OR})_{10}$ and $\text{Mo}_6\text{O}_{10}(\text{O-i-Pr})_{12}$ have been isolated and characterized. $[\text{Mo}(\text{OR})_4]_x$ compounds react with O_2 to give $\text{MoO}(\text{OR})_4$ compounds where R = t-Bu, x		

$x = 1$; $R = i\text{-Pr}$, $x = 2$ and $R = \text{CH}_2\text{-t-Bu}$, $x \geq 2$. $\text{Mo}(\text{O-t-Bu})_4$ and O_2 also react to yield $\text{MoO}_2(\text{O-t-Bu})_2$ and 2 t-BuO^\bullet . A general scheme for the reaction of $\text{Mo}_2(\text{OR})_6$ compounds with O_2 is proposed involving an initial facile cleavage of the $\text{Mo}\equiv\text{Mo}$ bond to give $\text{MoO}_2(\text{OR})_2$ and $\text{Mo}(\text{OR})_4$ compounds. The subsequent course of the reaction depends on the reactivity of $\text{Mo}(\text{OR})_4$ compounds. The new oxo-alkoxides $\text{MoO}_2(\text{O-t-Bu})_2$, $\text{MoO}_2(\text{OR})_2(\text{bpy})_2$, where $R = i\text{-Pr}$ and $\text{CH}_2\text{-t-Bu}$, $\text{Mo}_3(\mu_3\text{-O})(\mu_3\text{-OR})(\mu_2\text{-OR})_3(\text{OR})_6$, where $R = i\text{-Pr}$ and $\text{CH}_2\text{-t-Bu}$, $\text{Mo}_4\text{O}_8(\text{O-i-Pr})_4(\text{py})_2$ and $\text{Mo}_6\text{O}_{10}(\text{O-i-Pr})_{12}$ have been characterized by a variety of physico-chemical techniques. The oxo groups are formed from the added molecular oxygen. Crystal data for (i) $\text{MoO}_2(\text{O-i-Pr})_2(\text{bpy})_2 \cdot (\text{toluene})_{1/2}$ at -161°C , $a = 13.907(6) \text{ \AA}$, $b = 8.413(3) \text{ \AA}$, $c = 19.999(8) \text{ \AA}$, $\alpha = 111.02(1)^\circ$, $\beta = 71.37(2)^\circ$, $\gamma = 88.98(1)^\circ$, $Z = 4$, $d_{\text{calcd}} = 1.455 \text{ g cm}^{-3}$ in space group $P1$; (ii) $\text{Mo}_3\text{O}(\text{OCH}_2\text{-t-Bu})_{10} \cdot (\text{CH}_2\text{Cl}_2)_{1/3}$ at -161°C , $a = 35.557(19) \text{ \AA}$, $b = 18.969(9) \text{ \AA}$, $c = 19.342(9) \text{ \AA}$, $Z = 8$, $d_{\text{calcd}} = 1.283 \text{ g cm}^{-3}$, in space group $Pbcn$; (iii) $\text{Mo}_3\text{O}(\text{O-i-Pr})_{10}$ at -162°C , $a = 21.274(6) \text{ \AA}$, $b = 21.808(5) \text{ \AA}$, $c = 10.207(2) \text{ \AA}$, $\alpha = 98.69(1)^\circ$, $\beta = 92.92(1)^\circ$, $\gamma = 118.03(1)^\circ$, $Z = 4$, $d_{\text{calcd}} = 1.452 \text{ g cm}^{-3}$, in space group $P1$; (iv) $\text{Mo}_6\text{O}_{10}(\text{O-i-Pr})_{12}$ at -162°C , $a = 13.082(3) \text{ \AA}$, $b = 11.478(2) \text{ \AA}$, $c = 9.760(2) \text{ \AA}$, $\alpha = 106.40(1)^\circ$, $\beta = 91.85(1)^\circ$, $\gamma = 99.81(1)^\circ$, $Z = 1$, $d_{\text{calcd}} = 1.738 \text{ g cm}^{-3}$ in space group $P1$.

Accession For	
NTIS	<input checked="" type="checkbox"/>
GRA&I	<input type="checkbox"/>
DTIC TAB	<input type="checkbox"/>
Unannounced	<input type="checkbox"/>
Justification	
By	
Distribution/	
Availability Codes	
Dist	Avail and/or Special
A	



INTRODUCTION

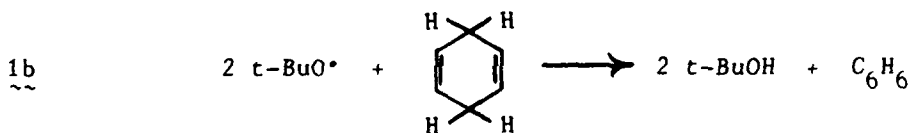
We have previously shown that the Mo=Mo bond in $\text{Mo}_2(\text{OR})_6$ compounds is labile toward a number of oxidative-addition reactions. Treatment with halogens leads to the formation of $\text{Mo}_2(\text{OR})_6\text{X}_4$ (M-M) compounds (R = i-Pr, X = Cl, Br and I), and addition of ROOR to formation of $\text{Mo}_2(\text{OR})_8$ (R = i-Pr).² Reaction with benzoyl peroxide gave³ a compound $\text{Mo}_2(\text{OR})_6(\text{O}_2\text{CPh})_2$ (R = i-Pr), believed to contain a Mo=Mo bond. These earlier findings prompted us to continue to investigate oxidative-additions with simple X_2 molecules. We report here our studies involving molecular oxygen. ~~Preliminary~~ reports of certain aspects of this work have been published.⁴⁻⁶

RESULTS AND DISCUSSION

Studies of the Reaction Between $\text{Mo}_2(\text{OR})_6$ and O_2 . We have limited our studies to reactions where R = t-Bu, i-Pr and CH_2 -t-Bu. These three alkoxides are taken to be representative primary, secondary and tertiary alkoxides for $\text{Mo}_2(\text{OR})_6$ compounds, bearing in mind that steric bulk is required in order to suppress oligomerization to $[\text{Mo}(\text{OR})_3]_x$.⁷

$\text{Mo}_2(\text{O-t-Bu})_6 + \text{O}_2$. Orange hydrocarbon solutions of $\text{Mo}_2(\text{O-t-Bu})_6$ fade slowly to pale yellow when stirred under one atmosphere of dry molecular oxygen. From experiments employing a gas buret, the moles of O_2 consumed per mole of $\text{Mo}_2(\text{O-t-Bu})_6$ is 2.0 ± 0.1 . Upon stripping the solvent, a thick yellow liquid remains which can be distilled at $50-55^\circ\text{C}$, 10^{-4} torr. Elemental analyses and all other characterization data indicate the yellow liquid is $\text{MoO}_2(\text{O-t-Bu})_2$. When $\text{Mo}_2(\text{O-t-Bu})_6$ is dissolved in benzene- d_6 or toluene- d_8 and sealed in an NMR tube under an atmosphere of O_2 , the ^1H NMR

spectrum shows that $\text{MoO}_2(\text{O-t-Bu})_2$ and t-BuOD are present in the molar ratio 2:1, respectively. The formation of t-BuOD was confirmed by two methods. (i) The NMR tube was opened and an authentic sample of t-BuOH was added. (ii) The volatile components were vacuum distilled into another NMR tube. t-BuOD was the only organic product observed by ^1H NMR spectroscopy. In related NMR tube reactions, $\text{Mo}_2(\text{O-t-Bu})_6$ and O_2 were allowed to react in toluene- d_8 in the presence of 1,4-cyclohexadiene. In these experiments, t-BuOH and benzene were the only organic products. Thus, the stoichiometry of the reaction shown in 1 is determined.



When $\text{Mo}_2(\text{O-t-Bu})_6$ and O_2 were allowed to react in a ca. 1:1 mole ratio, only unreacted $\text{Mo}_2(\text{O-t-Bu})_6$ and $\text{MoO}_2(\text{O-t-Bu})_2$, t-BuOH/D were detected by NMR spectroscopy. No intermediates have been detected in this reaction. Reactions involving $^{18}\text{O}_2$ yield $\text{Mo}^{18}\text{O}_2(\text{O-t-Bu})_2$, thereby establishing the origin of the oxo ligands.

$\text{Mo}_2(\text{O-i-Pr})_6 + \text{O}_2$. When hydrocarbon solutions of $\text{Mo}_2(\text{O-i-Pr})_6$ are stirred under one atmosphere of dry molecular oxygen, the color changes from yellow to green to brown and ultimately to pale yellow again. From experiments employing a gas buret, two equivalents of O_2 are consumed per equivalent of $\text{Mo}_2(\text{O-i-Pr})_6$ over the entire reaction sequence. Although the ultimate product $\text{MoO}_2(\text{O-i-Pr})_2$ is not easily isolated, being prone to

apparent autocatalytic decomposition to molybdenum blue oxides, the addition of 2,2'-bipyridine, bpy, after the uptake of two equivalents of O_2 , allows the isolation of the Lewis base adduct $MoO_2(O-i-Pr)_2(bpy)$. When $Mo_2(O-i-Pr)_6$ was dissolved in benzene- d_6 and allowed to react with O_2 , the organic volatiles were identified as *i*-PrOH and Me_2CO by 1H NMR spectroscopy and confirmed by the further addition of an authentic sample of each component. When a similar reaction was carried out in the presence of 1,4-cyclohexadiene, only *i*-PrOH and benzene were detected. Evidently, proton abstraction from 1,4-cyclohexadiene is favored over the bimolecular reaction of two *i*-PrO radicals, which gives *i*-PrOH and Me_2CO . The intermediates whose colors are observed prior to complete conversion to $MoO_2(O-i-Pr)_2$ are $Mo_3O(O-i-Pr)_{10}$ (green) and $Mo_6O_{10}(O-i-Pr)_{12}$ (dark yellow or brown). Both compounds were first isolated from reactions between $Mo_2(O-i-Pr)_6$ and less than two equiv of O_2 by crystallization.

Hydrocarbon solutions of $Mo_2(O-i-Pr)_6$, when treated with O_2 in the presence of added pyridine, initially turn red and then yellow as a relatively small quantity of red crystals are formed. The major products are $MoO_2(O-i-Pr)_2(py)_2$ and *i*-PrOH; $MoO(O-i-Pr)_4(py)$ and the red crystalline precipitate $Mo_4O_8(O-i-Pr)_4(py)_4$ are the minor products in this reaction. No $Mo_3O(O-i-Pr)_{10}$ is formed when pyridine is present.

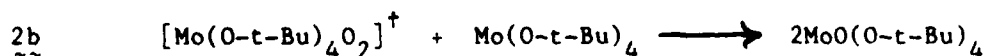
$Mo_2(OCH_2-t-Bu)_6 + O_2$. Hydrocarbon solutions of $Mo_2(OCH_2-t-Bu)_6$ change from yellow to green when treated with dry molecular oxygen. From experiments employing a gas buret, somewhat less than 2.0 equivalents (ca. 1.8) of O_2 are consumed per equivalent of $Mo_2(OCH_2-t-Bu)_6$. The major inorganic compound formed in this reaction is $MoO_2(OCH_2-t-Bu)_2$ which has

been isolated as an adduct with bpy, $\text{MoO}_2(\text{OCH}_2\text{-t-Bu})_2(\text{bpy})$, by the addition of bpy after the uptake of molecular oxygen had ceased. $\text{t-BuCH}_2\text{OH/D}$ is the organic product which was identified by analogous techniques to those described before in the detection of t-BuOH and i-PrOH . A minor residual product, $\text{MoO}(\text{OCH}_2\text{-t-Bu})_4$ has been detected by ^1H NMR spectroscopy and is probably responsible for the overall consumption of less than two equivalents of O_2 . The green compound, $\text{Mo}_3\text{O}(\text{OCH}_2\text{-t-Bu})_{10}$, has been shown to be formed early in the reaction.

When molecular oxygen is allowed to react with $\text{Mo}_2(\text{OCH}_2\text{-t-Bu})_6$ in the presence of pyridine, $\text{MoO}_2(\text{OCH}_2\text{-t-Bu})_2(\text{py})_2$ and $\text{t-BuCH}_2\text{OH}$ are the only products formed. No $\text{Mo}_3\text{O}(\text{OCH}_2\text{-t-Bu})_{10}$ was detected.

The aforementioned findings led us to suspect that Mo(IV) alkoxides, $[\text{Mo}(\text{OR})_4]_x$, might be involved as reactive intermediates in the reactions involving $\text{Mo}_2(\text{OR})_6$ compounds and O_2 .

Reactions of $[\text{Mo}(\text{OR})_4]_x$ Compounds with O_2 . $\text{Mo}(\text{O-t-Bu})_4 + \text{O}_2$. When hydrocarbon solutions of $\text{Mo}(\text{O-t-Bu})_4$ are exposed to an atmosphere of O_2 , the products depend upon the initial concentration of the Mo(IV) alkoxide. $\text{MoO}(\text{O-t-Bu})_4$ is the major product from concentrated solutions of $\text{Mo}(\text{O-t-Bu})_4$ (> 0.25 M), while $\text{MoO}_2(\text{O-t-Bu})_2$ and t-BuOH are the products from dilute solutions (< 0.001 M). A very plausible interpretation of this concentration effect may be based on the reactions shown in eq. 2.

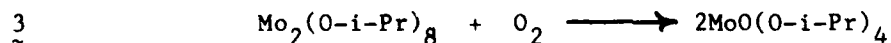




At high initial $\text{Mo}(\text{O}-t\text{-Bu})_4$ concentrations, the bimolecular pathway, $\underline{2b}$, leading to $\text{MoO}(\text{O}-t\text{-Bu})_4$ is favored. Dilute solutions of $\text{Mo}(\text{O}-t\text{-Bu})_4$ suppress the bimolecular pathway, $\underline{2b}$, and the products result from decomposition of the proposed dioxygen adduct, $[\text{Mo}(\text{O}-t\text{-Bu})_4\text{O}_2]$.

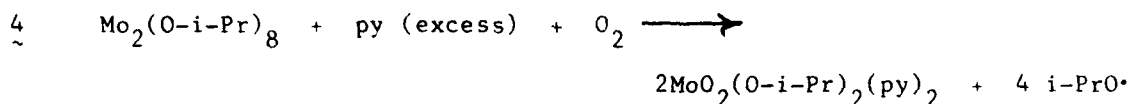
The steps proposed in $\underline{2}$ are similar to those proposed for oxygenation of a number of inorganic compounds. For example, Lever⁹ has shown that $\text{PcMn}(\text{O}_2)$, where Pc = phthalocyanine, forms when solutions of $\text{PcMn}(\text{II})$ are exposed to O_2 . Excess $\text{PcMn}(\text{II})$ reacts with the oxygen adduct to form $\text{PcMn}-\text{O}_2\text{-MnPc}$, which cleaves to give two equivalents of PcMnO . Likewise, Balch¹⁰ has shown that PFe , where P = a porphyrin dianion, forms a dimer when exposed to O_2 . The dimer then cleaves to form the mononuclear complex PFeO . Ledon¹¹ reported the formation of a cis-dioxo complex, MoO_2TPP , where TPP = tetraphenylporphyrin dianion, from a peroxo compound, $\text{Mo}(\text{O}_2)\text{-TPP}$. The latter compound was generated by photolysis of a diperoxy molybdenum porphyrin $\text{Mo}(\text{O}_2)_2\text{TPP}$.

$\underline{\text{Mo}_2(\text{O}-i\text{-Pr})_8(\text{M}=\text{M}) + \text{O}_2}$. Hydrocarbon solutions of $\text{Mo}_2(\text{O}-i\text{-Pr})_8$ react very rapidly with molecular oxygen to cleave the M-M double bond¹² and form two equivalents of $\text{MoO}(\text{O}-i\text{-Pr})_4$ according to equation $\underline{3}$.

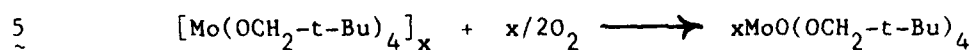


The stoichiometry of the uptake of O_2 was determined by experiments employing a gas buret. Reaction $\underline{3}$ is a metathesis reaction: M-M and O-O bonds react to give two M=O bonds.

When $\text{Mo}_2(\text{OPr}^i)_8$ is dissolved in pyridine, the blue color, which is believed to be associated with the Mo=Mo bond, disappears yielding a brown solution which is paramagnetic. $\text{Mo}(\text{O-i-Pr})_4(\text{py})_2$ is believed to be formed and is probably closely related to the well characterized compounds $\text{Mo}(\text{OSiR}_3)_4(\text{HNMe}_2)_2$, where $\text{R} = \text{Me}$ and Et .⁸ The reaction between $\text{Mo}_2(\text{O-i-Pr})_8$ dissolved in pyridine, $[\text{Mo}(\text{O-i-Pr})_4(\text{py})_2]$, and molecular oxygen proceeds according to equation 4. The isopropoxy radicals decompose to i-PrOH and Me_2CO as noted before.



$[\text{Mo}(\text{OCH}_2\text{-t-Bu})_4]_x + \text{O}_2$. Whether $\text{Mo}(\text{OCH}_2\text{-t-Bu})_4$ is a dimer or higher polymer in solution is not clear from magnetic and cryoscopic molecular weight data.⁸ However, hydrocarbon solutions of $[\text{Mo}(\text{OCH}_2\text{-t-Bu})_4]_x$ react rapidly with O_2 to yield $\text{MoO}(\text{OCH}_2\text{-t-Bu})_4$ according to the stoichiometric reaction 5. Uptake of O_2 was determined by gas buret experiments.



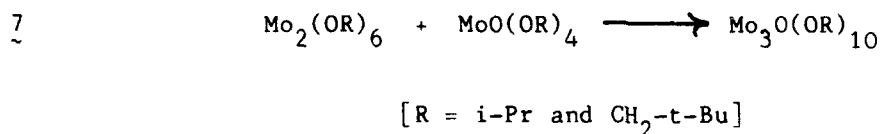
Alternate Syntheses of New Oxo-Alkoxides. $\text{MoO}_2(\text{OR})_2$ ($\text{R} = \text{i-Pr}$ and $\text{CH}_2\text{-t-Bu}$). Undoubtedly the quickest and cleanest syntheses of $\text{MoO}_2(\text{OR})_2$ compounds ($\text{R} = \text{i-Pr}$ and $\text{CH}_2\text{-t-Bu}$) is by the alcoholysis reaction shown in

6.



This avoids the slow reactions of the intermediates $\text{Mo}_3\text{O}(\text{OR})_3$ and $\text{Mo}_6\text{O}_{10}(\text{O}-i\text{-Pr})_{12}$ with O_2 when the $\text{Mo}_2(\text{OR})_6$ compounds are used.

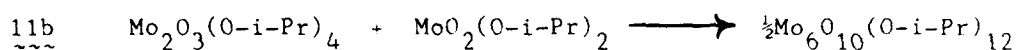
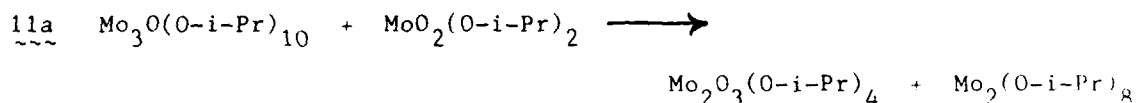
$\text{Mo}_3\text{O}(\text{OR})_{10}$ (R = i-Pr and $\text{CH}_2-t\text{-Bu}$). These compounds contain a triangulo $\text{Mo}_3(12+)$ unit capped by an oxo and an alkoxy ligand. A straightforward and quantitative synthesis of these compounds is according to 7.



This synthesis has an analogy with the assembly of small clusters employing $\text{M}=\text{CR}_2$ and $\text{M}=\text{CR}$ groups which has been exploited very successfully by Stone and coworkers.¹³ In 7, the six electrons of the $\text{Mo}=\text{Mo}$ bond are redistributed to form three $\text{Mo}-\text{Mo}$ single bonds ($a^2 + e^4$).

Reaction 7 is greatly influenced by the steric bulk of the R groups and by the choice of solvent. In pyridine or even hydrocarbon solutions containing pyridine, $\text{Mo}_2(\text{OR})_6$ and $\text{MoO}(\text{OR})_4$ do not react, presumably because pyridine coordinates to each and blocks the associative reaction. However, the compounds $\text{Mo}_3\text{O}(\text{OR})_{10}$ once formed are quite stable toward pyridine and other donor ligands. They do not dissociate to $\text{Mo}_2(\text{OR})_6$ and $\text{MoO}(\text{OR})_4$ compounds. The importance of steric factors is seen in the fact that $\text{Mo}_2(\text{O}-t\text{-Bu})_6$ and $\text{MoO}(\text{O}-t\text{-Bu})_4$ do not react; similarly, $\text{Mo}_2(\text{O}-i\text{-Pr})_6$ does not react with $\text{MoO}(\text{O}-t\text{-Bu})_4$, nor does $\text{Mo}_2(\text{O}-t\text{-Bu})_6$ react with $\text{MoO}(\text{O}-i\text{-Pr})_4$.

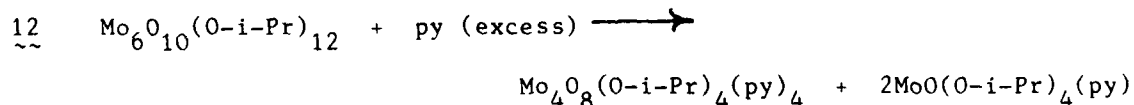
In reaction 9, the triangulo $\text{Mo}_3(12+)$ complex acts as a reducing agent and a similar sequence shown in 11 can be envisaged to give rise to $\text{Mo}_6\text{O}_{10}(\text{O-i-Pr})_{12}$.



$\text{Mo}_2(\text{O-i-Pr})_8$, formed in 11a, would react with $\text{MoO}_2(\text{O-i-Pr})_2$ to give $\text{Mo}_6\text{O}_{10}(\text{O-i-Pr})_{12}$ by the sequence shown in 10.

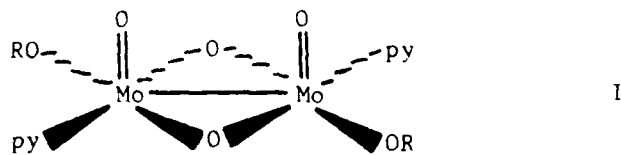
Related oxygen atom transfer reactions have been previously documented. For example, $\text{MoO}_2(\text{acac})_2$ and $\text{MoCl}_2(\text{acac})_2$ react¹⁴ to give $\text{MoOCl}(\text{acac})$, and $\text{W}(\text{CO})(\text{C}_2\text{H}_2)(\text{S}_2\text{CNR}_2)_2$ and $\text{Mo}_2\text{O}_3(\text{S}_2\text{P}(\text{OEt})_2)_4$ react¹⁵ to yield $\text{WO}(\text{C}_2\text{H}_2)(\text{S}_2\text{CNR}_2)_2$ and $\text{MoO}(\text{S}_2\text{P}(\text{OEt})_2)_2$ (2 equiv) with the liberation of CO.

$\text{Mo}_4\text{O}_8(\text{O-i-Pr})_4(\text{py})_4$. The $\text{Mo}_4\text{O}_8(\text{O-i-Pr})_4(\text{py})_4$ cluster is synthesized in high yield by the addition of pyridine to a toluene solution of $\text{Mo}_6\text{O}_{10}(\text{O-i-Pr})_{12}$, eq. 12.

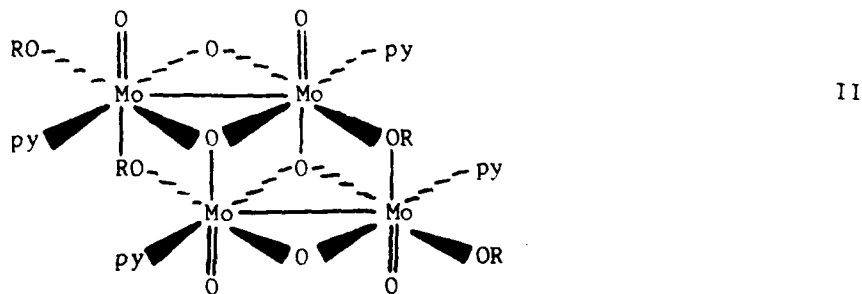


When this reaction is carried out in an NMR tube using toluene- d_8 as solvent, the $\text{Mo}_4\text{O}_8(\text{O-i-Pr})_4(\text{py})_4$ cluster precipitates from solution and $\text{MoO}(\text{O-i-Pr})_4(\text{py})$ is the only species detectable by NMR spectroscopy.

As is discussed subsequently, $\text{Mo}_6\text{O}_{10}(\text{O-i-Pr})_{12}$ is extensively dissociated in solution (benzene, toluene). Since the solutions remain diamagnetic, we propose that chain cleavage occurs with retention of the Mo-Mo single bonds. From a consideration of the structure of $\text{Mo}_6\text{O}_{10}(\text{O-i-Pr})_{12}$, it is easy to envisage a reaction with pyridine in which the two terminal molybdenum atoms form $\text{MoO}(\text{O-i-Pr})_4(\text{py})$ and the central portion of the molecule forms two equivalents of I.

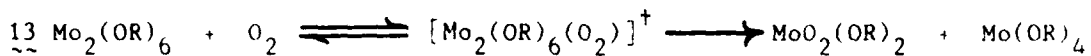


Two molecules of I may then associate to give II with the formation of two μ_3 -oxo groups and two μ_2 -OR groups. The square based pyramidal coordination for molybdenum in I is transformed to octahedral coordination in II, but with retention of the Mo-Mo single bonds.



$\text{Mo}_2(\text{OR})_6 + \text{O}_2$: A General Reaction Scheme. It is possible to envisage an overall scheme of reactions involving $\text{Mo}_2(\text{OR})_6$ compounds and molecular

oxygen leading to $\text{MoO}_2(\text{OR})_2$ compounds based on an initial facile cleavage of the $\text{Mo}\equiv\text{Mo}$ bond, eq. 13.



It may be noted that a number of other small molecules, CO and $\text{HC}\equiv\text{CH}$, react with $\text{Mo}_2(\text{OR})_6$ compounds to form reactive 1:1 adducts.^{16,17} Disproportionation reactions have been observed and from the reaction between $\text{Mo}_2(\text{O}-t\text{-Bu})_6$ and CO, $\text{Mo}(\text{O}-t\text{-Bu})_4$ has been isolated.¹⁸

The $\text{Mo}(\text{OR})_4$ molecule formed in 13 may react in a number of ways. (1) It may react with O_2 as outlined in 2a, 2b and 2c. (2) It may associate to form $\text{Mo}_2(\text{O}-i\text{-Pr})_8$ or $[\text{Mo}(\text{OCH}_2-t\text{-Bu})_4]_x$, which then may react with O_2 to give $\text{MoO}(\text{OR})_4$ compounds. Alternatively, $[\text{Mo}(\text{OR})_4]_x$ may react with $\text{MoO}_2(\text{OR})_2$ to give $\text{Mo}_6\text{O}_{10}(\text{O}-i\text{-Pr})_{12}$ and $\text{MoO}(\text{O}-i\text{-Pr})_4$, eq. 9. (3) The $\text{MoO}(\text{OR})_4$ compounds may react with $\text{M}_2(\text{OR})_6$ to yield $\text{Mo}_3\text{O}(\text{OR})_{10}$ compounds, when R = *i*-Pr and $\text{CH}_2-t\text{-Bu}$. However, in the absence of reduced molybdenum alkoxides, $\text{MoO}(\text{OR})_4$ compounds become ultimate products along with $\text{MoO}_2(\text{OR})_2$ compounds. (4) $\text{Mo}_3\text{O}(\text{OR})_{10}$ compounds (R = *i*-Pr and $\text{CH}_2-t\text{-Bu}$) react directly with O_2 , leading to $\text{RO}\cdot$ and $\text{MoO}_2(\text{OR})_2$. [This reaction remains to be studied in detail.] $\text{Mo}_3\text{O}(\text{OR})_{10}$ compounds also react with $\text{MoO}_2(\text{OR})_2$ compounds to give $\text{Mo}_6\text{O}_{10}(\text{O}-i\text{-Pr})_{12}$ which, being dissociatively labile, may be viewed as a source of two $\text{MoO}(\text{O}-i\text{-Pr})_4$ molecules and two $\text{Mo}_2\text{O}_4(\text{O}-i\text{-Pr})_2$ fragments. (5) $\text{Mo}_6\text{O}_{10}(\text{O}-i\text{-Pr})_{12}$, which contains two Mo-Mo single bonds, behaves as a four-electron reductant in a final reaction with O_2 , yielding $\text{MoO}_2(\text{O}-i\text{-Pr})_2$.

A number of qualitative statements concerning relative rates and product distributions can be made based on steric factors of the RO ligands which greatly influence the fate of the Mo(IV) alkoxy intermediates. However, these are speculative and are not presented here.

Characterization of Oxo-Alkoxy-Molybdenum Compounds. Some fundamental characterization properties of the oxo-alkoxy-molybdenum compounds are reported in Table I. Analytical data are given in Table II. ^1H NMR data and ^{17}O chemical shifts for representative terminal oxo groups are given in Table III. Stretching frequencies for terminal Mo=O groups are given in Table IV. Other characterization data are recorded in the Experimental Section or discussed in the following sections.

Solution and Physicochemical Properties of Mo(6+) Compounds. $\text{MoO}_2(\text{O-t-Bu})_2$ is a yellow liquid, distillable at 55°C , 10^{-4} torr. It is stable under a dry atmosphere of oxygen or nitrogen, but quickly decomposes to blue molybdenum oxides when exposed to moisture. The ^{17}O and ^1H NMR spectra indicate only one type of oxo and alkoxy group are present in the molecule. The ^{17}O chemical shift of the oxo-ligand, 862 ppm downfield from H_2^{17}O , is well within the range of terminal oxo ligands for Mo(6+) containing compounds.¹⁹ The peak width at half height for the ^{17}O signal at 862 ppm is 90 Hz, indicative of a monomeric species in solution.¹⁹ This is also confirmed by a cryoscopic molecular weight determination in benzene. In the infrared spectrum, $\text{MoO}_2(\text{O-t-Bu})_2$ shows two bands at 968 and 930 cm^{-1} , assignable to antisymmetric and symmetric Mo=O stretches, respectively. Upon ^{18}O labelling ($\text{Mo}_2(\text{O-t-Bu})_6 + ^{18}\text{O}_2 + \text{Mo}^{18}\text{O}_2(\text{O-t-Bu})_2$),

these bands shift to 920 and 887 cm^{-1} , respectively. $\text{MoO}_2(\text{O}-t\text{-Bu})_2$ is therefore formulated as a molecule with virtual C_{2v} symmetry; it may be thought of as a dialkylated derivative of MoO_4^{2-} , namely the tert-butyl ester of molybdic acid.

$\text{MoO}_2(\text{OR})_2$, where $\text{R} = i\text{-Pr}$ and $\text{CH}_2-t\text{-Bu}$ are white solids which are only sparingly soluble in pentane and hexane. When crystallized from either solvent, filtered, and dried in vacuo, they decompose to blue molybdenum oxides. They can be kept in hydrocarbon solutions for a much longer time without decomposition, however.

$\text{MoO}_2(\text{OR})_2(\text{py})_2$ and $\text{MoO}_2(\text{OR})_2(\text{bpy})$, where $\text{R} = i\text{-Pr}$ and $\text{CH}_2-t\text{-Bu}$. The pyridine adducts of $\text{MoO}_2(\text{OR})_2$ are yellow liquids which lose pyridine upon heating under vacuum. Their spectroscopic properties indicate that they have essentially the same MoO_4N_2 geometry found for the related bpy adducts.

$\text{MoO}_2(\text{OR})_2(\text{bpy})$ compounds ($\text{R} = i\text{-Pr}$ and $\text{CH}_2-t\text{-Bu}$) are white, air-sensitive solids which are soluble in chlorocarbon solvents, but only sparingly soluble in hydrocarbon solvents.

^{17}O NMR spectra for $\text{MoO}_2(\text{OR})_2(\text{py})_2$ and $\text{MoO}_2(\text{OR})_2(\text{bpy})$ show only one signal in the range of terminal oxo groups and the line width is sufficiently narrow to indicate monomeric species.

Kidd²⁰ has shown that, for a series of oxo-chromium(6+) compounds, a linear correlation exists between $\text{M}-\text{O}$ π bond order and ^{17}O chemical shift: increasing π bond order increases the paramagnetic screening of the oxygen nucleus and results in a larger chemical shift (relative to H_2^{17}O).

Reilly²¹ demonstrated that a non-linear correlation exists between ^{17}O chemical shifts and Mo-O bond distances ranging from 1.6 to 2.4 Å, but over the narrower range of terminal Mo-oxo distances, 1.6 to 1.9 Å, Wentworth and Miller²² have proposed a linear correlation between chemical shift and Mo-O bond distance. According to the Wentworth-Miller correlation, the ^{17}O chemical shift found for $\text{MoO}_2(\text{O-i-Pr})_2(\text{bpy})_2$ leads to a predicted Mo-O (oxo) distance of 1.71 Å which agrees well with the average distance found in the solid state structure.

It should also be noted that the ^{17}O chemical shifts for $\text{MoO}_2(\text{OR})_2(\text{py})_2$ and $\text{MoO}_2(\text{OR})_2(\text{bpy})$ compounds are smaller than those of other octahedral cis-MoO_2^{2+} containing compounds, e.g. $\text{MoO}_2(\text{acac})_2$ (1025) and $\text{MoO}_2(\text{S}_2(\text{CNEt}_2)_2)$ (975).²² This implies somewhat less oxo-molybdenum π -bonding in $\text{MoO}_2(\text{OR})_2(\text{bpy})$ compounds than the maximum π bond order of 1.5 which is possible for a cis-MoO_2^{2+} containing compound. According to a Miller-Wentworth plot of π bond order versus ^{17}O chemical shift, a π bond order of 1.37 per Mo-oxo bond is determined for $\text{MoO}_2(\text{OR})_2(\text{py})_2$ and $\text{MoO}_2(\text{OR})_2(\text{bpy})_2$ compounds. Apparently, the alkoxy groups are also competing as π donor ligands. This is supported by considerations of oxo and alkoxy Mo-O bond distances discussed later.

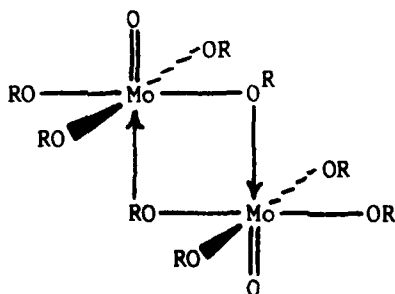
Solid State Molecular Structure of $\text{MoO}_2(\text{O-i-Pr})_2(\text{bpy})$. An ORTEP view of the $\text{MoO}_2(\text{O-i-Pr})_2(\text{bpy})$ molecule is shown in Figure 1. Atomic coordinates are given in Table V. Selected bond distances and bond angles are reported in Tables VI and VII. Anisotropic thermal parameters and complete listings of bond distances and angles are available in the supplementary material.

The molecule has virtual C_{2v} symmetry. The geometry about molybdenum is a distorted octahedral one. All of the distortions are easily understood. The oxo-Mo-oxo angle of 108° arises from the repulsive interactions of the cis multiple bonds. These forces also operate to bend the mutually trans O-i-Pr ligands away from the O-O edge of the octahedron. The planar bpy ligand, with its small bite, 69° , easily accommodates this distortion. The Mo-O (oxo) distance, 1.71 \AA (averaged), is slightly longer than those typically found for terminal cis-MoO_2^{2+} compounds, 1.68 \AA , which is consistent with the view, previously expressed as a result of the ^{17}O chemical shift data, that the maximum oxo-Mo π bond order is not attained because of RO-to-Mo π -bonding. The Mo-O (alkoxy) distance, 1.93 \AA (averaged), is sufficiently short to be suggestive of some alkoxy-to-molybdenum π -bonding.²⁴ It is, however, notably longer than the Mo-OR (terminal) distance, 1.81 \AA (averaged), found in $\text{Mo}_2(\text{O-i-Pr})_6\text{X}_4$ compounds (X = Cl, Br),² where RO-to-Mo π -bonding does not have to compete with other strong π -donor ligands. The Mo-N (bpy) distance, 2.34 \AA (averaged), is long, presumably because of the high trans-influence of the trans oxo ligands.²⁵ The C-C and C-N distances of the bpy ligand are normal and an interesting comparison with the short Mo-N and distorted bpy C-C and C-N distances found in the $\text{Mo}(\text{O-i-Pr})_2(\text{bpy})_2$ molecule will be made elsewhere.²⁶

The ability of the $\text{MoO}_2(\text{O-i-Pr})_2$ unit to coordinate bpy leads to the expectation that $\text{MoO}_2(\text{OR})_2$ compounds, where R = i-Pr and $\text{CH}_2\text{-t-Bu}$, are polymeric in the solid state.

MoO(OR)₄ Compounds. $\text{MoO}(\text{O-t-Bu})_4$ and $\text{MoO}(\text{O-i-Pr})_4$ are yellow liquids which can be vacuum distilled. $\text{MoO}(\text{OCH}_2\text{-t-Bu})_4$ is a yellow solid which can

be sublimed in vacuum and crystallized from toluene or hexane solutions. All three compounds are stable under a dry oxygen or nitrogen atmosphere, but quickly decompose to give blue molybdenum oxides when exposed to moisture. The ^{17}O and ^1H NMR spectra indicate only one type of oxo ligand and one type of OR ligand, respectively. The ^{17}O chemical shift values are within the range expected for terminal oxo groups bonded to $\text{Mo}(6+)$.¹⁹ Cryoscopic molecular weight determinations in benzene on $\text{MoO}(\text{O}-i\text{-Pr})_4$ and $\text{MoO}(\text{OCH}_2\text{-}t\text{-Bu})_4$ show that they are predominantly monomeric in solution with observed (calculated) molecular weights of 410 ± 30 (348) and 499 ± 50 (460), respectively. Since the steric bulk of the alkoxide ligands is in the order $t\text{-BuO} > i\text{-PrO} > \text{CH}_2\text{-}t\text{-Bu}$,²⁷ the compound $\text{MoO}(\text{O}-t\text{-Bu})_4$ is almost certainly a monomer. Since the observed molecular weights are slightly higher than that of the monomer, it is likely that there is rapid monomer \rightleftharpoons dimer equilibrium in solution with the position of the equilibrium favoring the monomer. However, in the solid state, weak association through RO bridge formation could lead to octahedral coordination for molybdenum as shown in III. The infrared spectra (Nujol mulls) show terminal $\text{Mo}=\text{O}$ stretches at 967 , 951 and 915 cm^{-1} , for $\text{R} = t\text{-Bu}$, $i\text{-Pr}$ and $\text{CH}_2\text{-}t\text{-Bu}$, respectively.



III

The related compound $\text{MoO}(\text{OC}(\text{CF}_3)_3)_4$ has been prepared²⁸ from the reaction between MoOCl_4 and $\text{NaOC}(\text{CF}_3)_3$ in CH_2Cl_2 solvent. The molecular structure of this volatile yellow solid showed the central MoO_5 unit is a distorted square based pyramid with the oxo ligand in the apical position. A similar geometry is expected for $\text{MoO}(\text{O}-t\text{-Bu})_4$. The possibility that the $\text{MoO}(\text{OR})_4$ compounds, where $\text{R} = i\text{-Pr}$ and $\text{CH}_2-t\text{-Bu}$, are dimers can not be overlooked, however, and the molecular structure of $\text{Mo}_6\text{O}_{10}(\text{O}-i\text{-Pr})_{12}$, discussed later, may be viewed as the sum of two $\text{MoO}(\text{O}-i\text{-Pr})_4$ molecules associated to two $\text{Mo}_2\text{O}_4(\text{O}-i\text{-Pr})_2$ units. The lower values of $\nu(\text{Mo}=\text{O})$ for $\text{R} = i\text{-Pr}$ (951 cm^{-1}) and $\text{R} = \text{CH}_2-t\text{-Bu}$ (915 cm^{-1}) relative to $\nu(\text{Mo}=\text{O}) = 967 \text{ cm}^{-1}$ for $\text{R} = t\text{-Bu}$, may well reflect the formation of weak $\text{RO} \rightarrow \text{Mo}$ bonds trans to $\text{Mo}-\text{O}$ bonds in the former compounds.

Mass Spectra of Mo(6+) Oxo-Alkoxides: A General Scheme. The mass spectra of all the new Mo(6+) oxo-alkoxides were examined by the method of direct insertion using electron impact ionization. None of the new compounds showed a molecular ion. The bpy and pyridine adducts lose the Lewis base ligands in the vapor state. Hence, $\text{MoO}_2(\text{O}-t\text{-Bu})_2$, $\text{MoO}_2(\text{O}-t\text{-Bu})_2(\text{py})_2$ and $\text{MoO}_2(\text{O}-t\text{-Bu})_2(\text{bpy})$ all show identical fragmentation patterns for the metal containing ions. The ions of highest mass are shown in Table VIII.

$\text{MoO}_2(\text{O}-i\text{-Pr})_2(\text{bpy})$ was prepared using a variety of isotopic labels in order to assist in determining the fragmentation pattern. The mass spectrum of $\text{Mo}^{18}\text{O}_2(\text{O}-i\text{-Pr})_2(\text{bpy})$ is similar to that of $\text{MoO}_2(\text{O}-i\text{-Pr})_2(\text{bpy})$: all the metal-containing ions show an increase of four mass units. The oxo ligands are thus shown to be derived from molecular oxygen and oxo groups are not eliminated during mass spectral fragmentation. The fragmentation

is entirely due to the alkoxide ligands. For protio compounds, the ion of highest mass corresponds to M-15, and deuterio compounds show M-18, corresponding to loss of CH_3 and CD_3 , respectively. This is then followed by a loss of alkene by abstraction of H/D from a carbon atom beta to the alkoxide oxygen atom. This type of fragmentation has been seen before for other metal isopropoxides²⁹ and is summarized in Scheme 1 which shows the results of the pertinent labelling experiments.

$\text{MoO}_2(\text{O-t-Bu})_2(\text{bpy})$ follows the same pattern: initial loss of methyl from a tert-butoxy group is followed by elimination of iso-butylene from the other. A similar fragmentation is seen for $\text{Cr}(\text{O-t-Bu})_4$.³⁰

The $\text{MoO}(\text{OR})_4$ compounds fragment in a manner akin to that previously described for $\text{WO}(\text{O-t-Bu})_4$.³¹ Initial loss of an alkoxide ligand, followed by elimination of alkene, yields the ion fragments in the series: $\text{MoO}(\text{OR})_4^+ \rightarrow \text{MoO}(\text{OR})_3^+ \rightarrow \text{MoO}(\text{OH})(\text{OR})_2^+ \rightarrow \text{MoO}(\text{OH})_2(\text{OR})^+ \rightarrow \text{MoO}(\text{OH})_3^+$.

$\text{Mo}_3\text{O}(\text{OR})_{10}$ Compounds, where R = i-Pr and $\text{CH}_2\text{-t-Bu}$: Solution and Physico-Chemical Properties. The compounds $\text{Mo}_3\text{O}(\text{OR})_{10}$, where R = i-Pr and $\text{CH}_2\text{-t-Bu}$ are green crystalline solids which are indefinitely stable under a nitrogen atmosphere and in solution. They slowly react with molecular oxygen to form $\text{MoO}_2(\text{OR})_2$ compounds with the elimination of alkoxy radicals and they hydrolyze in the presence of moisture. They are soluble in aromatic and aliphatic hydrocarbons and methylene chloride, but insoluble and unreactive toward pyridine. The $\text{Mo}_3\text{O}(\text{OR})_{10}$ compounds decompose at temperatures above 100°C and could not be sublimed in vacuo. No metal containing ions were observed in the mass spectrometer.

^1H NMR spectra of $\text{Mo}_3\text{O}(\text{O-i-Pr})_{10}$ compounds are consistent with expectations based upon considerations of the molecular structures found in the solid state which have virtual C_{3v} symmetry. The presence of four types of alkoxy ligands in the ratio 3:3:3:1 shows that bridge-terminal exchange is not rapid on the NMR time-scale. The spectra are unaffected by added pyridine, indicating that bridging OR ligands cannot readily be displaced by donor ligands. No signal was observed in the natural abundance ^{17}O NMR spectrum and the preparation of $\text{Mo}_3^{18}\text{O}(\text{O-i-Pr})_{10}$ did not allow an assignment of $\nu(\text{Mo}_3-\mu_3-\text{O})$ by a comparison with the ^{16}O infrared spectrum.

A more detailed study of the electronic spectra and electrochemical behavior of these $\text{Mo}_3\text{O}(\text{OR})_{10}$ compounds is currently underway.

Solid State and Molecular Structures. Crystals of the neopentoxide were first examined and, while the structure was readily solved, a disorder problem associated with one of the neopentyl ligands (the μ_3 -OR ligand), a partial occupancy of a solvent molecule within the unit cell which refined to a 0.33 occupancy factor and the general rather high thermal vibrations associated with the neopentyl methyl groups, all contributed to a rather unsatisfactory characterization. Consequently, the isopropoxide was also examined. Atomic positional parameters are given for $\text{Mo}_3\text{O}(\text{OCH}_2\text{-t-Bu})_{10}$ and $\text{Mo}_3\text{O}(\text{O-i-Pr})_{10}$ in Tables IX and X, respectively.

In the space group $\text{P}\bar{1}$, there are two independent $\text{Mo}_3\text{O}(\text{O-i-Pr})_{10}$ molecules in the unit cell, differing only slightly with respect to the conformations of the isopropyl groups. A least squares fit of the $\text{Mo}_3\text{O}(\text{OC}_\alpha)_10$ skeletons of the $\text{Mo}_3\text{O}(\text{O-i-Pr})_{10}$ molecules to the $\text{Mo}_3\text{O}(\text{OC}_\alpha)_10$

skeleton of the $\text{Mo}_3\text{O}(\text{OCH}_2\text{-t-Bu})_{10}$ molecule was performed by fitting the three molybdenum atoms and then calculating the difference in positions of the unmatched atoms. The $\text{Mo}_3\text{O}(\text{OC}_\alpha)_{10}$ skeletons are virtually identical, with no oxygen atom differing by more than $0.21(1) \text{ \AA}$ and no C_α differing by more than $0.95(1) \text{ \AA}$. Comparisons of bond distances and bond angles for the central Mo_3O_{11} units of the three crystallographically independent $\text{Mo}_3\text{O}(\text{OR})_{10}$ molecules are given in Table XI and XII, respectively. An ORTEP view of the central Mo_3O_{11} skeleton showing the atom number scheme used for the three molecules is given in Figure 2. Tables listing anisotropic thermal parameters and complete listings of bond distances and angles, together with figures showing the atom number schemes, are given in the supplementary data. Two stereoviews of one of the $\text{Mo}_3\text{O}(\text{O-i-Pr})_{10}$ molecules are shown in Figure 3. These oxo-alkoxides of molybdenum are members of a now fairly extensive class of triangulo Mo_3 -containing compounds with either one or two capping ligands.³² The geometry of the oxo-alkoxide cluster is, however, different from any previously seen. The most pertinent comparisons are with the oxo capped clusters $\text{Mo}_3\text{O}_4(\text{C}_2\text{O}_4)_3(\text{H}_2\text{O})_3^{2+}$ and $\text{Mo}_3\text{O}_2(\text{O}_2\text{CMe})_3(\text{H}_2\text{O})_3^{2+}$ which contain central $\text{Mo}_3\text{O}_{13}^{33}$ and $\text{Mo}_3\text{O}_{17}^{34}$ skeletons, respectively. A comparison of the Mo_3O_{11} unit in $\text{Mo}_3\text{O}(\text{OR})_{10}$ compounds with the Mo_3O_{13} and Mo_3O_{17} skeletons is shown in Figure 4. The Mo_3O_{17} unit allows each molybdenum atom to be seven coordinate while, in both Mo_3O_{11} and Mo_3O_{13} , the molybdenum atoms are six coordinate, being in a roughly octahedral environment. The oxalate containing ion $\text{Mo}_3\text{O}_4(\text{C}_2\text{O}_4)_3(\text{H}_2\text{O})_3^{2+}$ has a Mo_3O_{13} unit with only one capping ligand and essentially the same unit is found in a number of ternary oxides of molybdenum having

formula $MM'Mo_3O_8$, where M and M' are two cations with charge totalling +4, e.g. Zn_2 or $LiSc$.³⁵⁻³⁷ One could imagine that the Mo_3O_{11} unit of $Mo_3O(OR)_{10}$ compounds could be converted to the Mo_3O_{13} unit by a Lewis base association reaction involving the addition of a pair of alkoxide ligands: $Mo_3O(OR)_{10} + 2NaOR + Na_2Mo_3O(OR)_{12}$. One might also imagine that a CO_2 insertion reaction,³⁸ or an acetate for OR exchange reaction, could convert the Mo_3O_{11} unit to the Mo_3O_{17} unit of $Mo_3O_2(OAc)_6(H_2O)_3^{2+}$: $Mo_3O(OR)_{10} + 6CO_2 + Mo_3(\mu_3-O)(\mu_3-OR)(\mu_2-OR)_3(O_2COR)_6$. These possibilities remain to be explored.

The following general observations concerning the $Mo_3O(OR)_{10}$ structures are worthy of note. (1) The average $Mo-O(\mu_3-OR)$ distance, 2.19(3) Å, is considerably longer than the average $Mo-\mu_3$ -oxo distance, 2.04(3) Å, as expected.²⁴ (2) The $Mo-O(\mu_2-OR)$ distances, 2.03(3) Å (averaged), are typical of $Mo-\mu_2-OR$ distances where there is a metal-metal bond.²⁴ (3) The $Mo-O$ distances to the terminal alkoxide ligands are short, 1.88(3) Å, and long, 1.95(3) Å, when they are trans to the capping alkoxide and oxo ligand, respectively. This presumably reflects the relative trans influence²⁵ $oxo > RO$. The $Mo-Mo$ distance, 2.53 Å (averaged) is similar to that in $Mo_3O_4(C_2O_4)_3(H_2O)_3^{2+}$, 2.49 Å, and that in $Zn_2Mo_3O_8$, 2.52 Å, and is indicative of $Mo-Mo$ single bonds in these types of triangulo Mo_3^{12+} -containing species. A ground state molecular orbital configuration for the $M-M$ bonds, $a^2 + e^4$, may be pictured to arise primarily from combinations of molybdenum atomic d_{z^2} and d_{xz} orbitals, where the z axis is defined as a vector from each molybdenum atom to the center of the Mo_3 triangle and the x axis is the plane of the triangle.

Further studies on these interesting $\text{Mo}_3\text{O}(\text{OR})_{10}$ compounds are planned.

$\text{Mo}_4\text{O}_8(\text{O-i-Pr})_4(\text{py})_4$. $\text{Mo}_4\text{O}_8(\text{O-i-Pr})_4(\text{py})_4$ is a red crystalline solid which is insoluble in aliphatic and aromatic hydrocarbon solvents. It is stable in the air for short periods of time, but slowly hydrolyses. $\text{Mo}_4^{18}\text{O}_8(\text{O-i-Pr})_4(\text{py})_4$ was prepared from the reaction between $\text{Mo}_2(\text{O-i-Pr})_6$ and $^{18}\text{O}_2$ in the presence of pyridine. A comparison of the infrared spectra of the ^{16}O and ^{18}O labelled compounds allows the assignment of $\nu(\text{Mo}-^{16}\text{O}) = 941$ and 918 cm^{-1} for terminal oxo groups and $\nu(\text{Mo}-^{16}\text{O}) = 727$ and 655 cm^{-1} for the bridging oxo ligands.

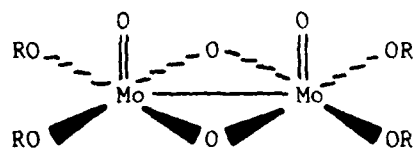
The molecular structure determined from an X-ray study has been previously described as part of a study of M-M bonding in compounds of formula $\text{M}_4(\mu_3\text{-X})_2(\mu_2\text{-X})_4\text{X}_{10}$.³⁹ The structure is represented as II and may be viewed as the product from dimerization of I shown earlier.

$\text{Mo}_6\text{O}_{10}(\text{O-i-Pr})_{12}$. Solution and Physicochemical Properties. $\text{Mo}_6\text{O}_{10}(\text{O-i-Pr})_{12}$ is a yellow-orange crystalline solid which is slightly soluble in aromatic solvents and essentially insoluble in aliphatic hydrocarbon solvents. The ^1H NMR spectrum in toluene- d_8 at $+16^\circ\text{C}$ shows broadened resonances for the O-i-Pr ligands but, at $+75^\circ\text{C}$, there is only a sharp septet and doublet. Evidently at $+75^\circ\text{C}$, there is rapid scrambling of all alkoxide ligands on the NMR time-scale. A cryoscopic molecular weight determination in benzene gave $M = 483 \pm 30$, which is much lower than that calculated for the hexanuclear formula. Evidently the Mo_6 chain is fragmented in benzene.

Solid State and Molecular Structure. The molecule $\text{Mo}_6\text{O}_{10}(\text{O-i-Pr})_{12}$ crystallized from toluene in the space group $\bar{P}1$ with one molecule in the unit cell. The molecule thus has a crystallographically imposed center of symmetry. An ORTEP view of the $\text{Mo}_6\text{O}_{10}(\text{O-i-Pr})_{12}$ molecule giving the atom number scheme used in the tables is shown in Figure 5. Atomic positional parameters are given in Table XIII and selected bond distances and angles are given in Table XIV and XV, respectively.

The six molybdenum atoms are, to within 0.01 \AA , all in the same plane. The metal-metal distances $\text{Mo}(1)\text{-Mo}(2) = \text{Mo}(1)'\text{-Mo}(2) = 2.585(1) \text{ \AA}$ are indicative of localized Mo-Mo single bonds, while the distances $\text{Mo}(2)\text{-Mo}(3) = \text{Mo}(2)'\text{-Mo}(3)' = 3.285(1) \text{ \AA}$ and $\text{Mo}(1)\text{-Mo}(1)' = 3.353(1) \text{ \AA}$ are typical of non-bonding distances between molybdenum atoms bridged by a pair of OR ligands.²⁴ The average oxidation state of molybdenum in $\text{Mo}_6\text{O}_{10}(\text{O-i-Pr})_{12}$ is +5.33 and, if charge is partitioned by counting a terminal oxo as -2, a bridging oxo as -1, a terminal OR as -1 and a bridging OR as $-\frac{1}{2}$ per metal, the oxidation states in the chain are $\text{Mo}(3) = \text{Mo}(3)' = +6$, $\text{Mo}(2) = \text{Mo}(2)' = \text{Mo}(1) = \text{Mo}(1)' = +5$. The Mo-Mo distances clearly indicate that the four electrons available for metal-metal bonding are used to form two localized M-M single bonds.

The centrosymmetric $\text{Mo}_6\text{O}_{10}(\text{O-i-Pr})_{12}$ molecule may be viewed as a dimer of $\text{Mo}_3\text{O}_5(\text{O-i-Pr})_6$, brought together through the agency of a pair of RO bridges. The $\text{Mo}_3\text{O}_5(\text{O-i-Pr})_6$ unit may be further broken down into $\text{MoO}(\text{O-i-Pr})_4$ and $\text{Mo}_2\text{O}_4(\text{O-i-Pr})_2$ units. While the latter is as yet unknown, when supported by alkoxy bridges as in IV, the fused square based pyramidal units are similar to scores of $\text{Mo}_2\text{O}_4^{2+}$ containing compounds.



IV

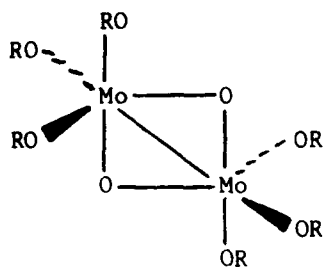
If the Mo-oxo vector is taken as the z axis and the M-L bonds are formed using metal s, p_x , p_y and $d_{x^2-y^2}$ atomic orbitals, the metal-metal bond is easily pictured from the interaction of the d_{xy} - d_{xy} orbitals. Oxygen-to-molybdenum π -bonding will use the d_{xz} and d_{yz} orbitals. Some pertinent distances found for the $\text{Mo}_2\text{O}_4^{2+}$ units in $\text{Mo}_6\text{O}_{10}(\text{O-i-Pr})_{10}$ and $\text{Mo}_4\text{O}_8(\text{O-i-Pr})_4(\text{py})_4$ are compared with those of other compounds in Table XVI.

As with other square based pyramidal molecules containing a multiple bond in the apical position, the molybdenum atoms lie above the basal plane of the four sigma bonded ligands. The coupling of two $\text{Mo}_2\text{O}_4(\text{OR})_2$ units in the head-to-tail manner thus produces a zig-zag for the four metal atoms. The S-curve is completed by attaching the two $\text{MoO}(\text{O-i-Pr})_4$ units such that one oxygen of an O-i-Pr ligand is tucked below the basal plane of its five-coordinate neighbor. The positioning of this group allows for incipient Mo-OR bond formation trans to the oxo-molybdenum bond. Indeed based on the following structural data, we suggest that this one alkoxide ligand is really "semi-bridging". (1) The terminal Mo(3)-OR distances are all within the range expected,²⁴ but the Mo(3)-O(12) distance of 1.919(2) Å is 0.05 Å longer than the others. (2) The Mo(2)---O(12) distance is 2.88(1) Å, too long to be called a bond, but much too short for a non-bonding interaction. (3) The Mo(3)-O(12)-C(24) angle is 127.5(1)°, indicative of sp^2 hybridization at O(12). While the

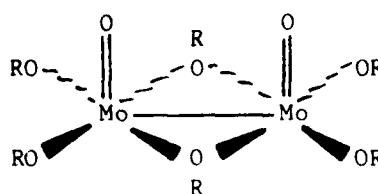
oxygen p_z atomic orbital may π -bond to Mo(3), the lone pair sp^2 orbital, which is contained in the Mo(3)-O(12)-C(24) plane is directed toward Mo(2). The Mo(2)---O(12)-C(24) angle is $83.9(1)^\circ$. If it is agreed that the O(12)---Mo(2) interaction is an attractive one, then this can contribute to the folding of the molecule. The Mo(3)-Mo(2)-Mo(1) angle, $134.3(1)^\circ$, is smaller than the Mo(2)-Mo(1)-Mo(1)' angle, $146.5(1)$.

The term "semi-bridging" is now commonly used in metal carbonyl chemistry where semi-bridging carbonyls may result from either electronic^{41,42} or steric factors.⁴³ Aside from the obvious difference that CO is a π -acceptor and RO is a π -donor ligand, the ligands share a number of common features including their abilities to act as bridging ligands (μ_2 and μ_3) and to support fluxional processes in solution, whereby bridging and terminal groups are exchanged rapidly on the NMR time scale. Though it is possible to envisage that the semi-bridging OR group is a result of steric factors, we feel it is more likely that the origin is electronic in nature. The five coordinate Mo(5+) atoms can readily increase their coordination number to six by ligation in the position trans to the oxo group. This is seen in the reaction of $Mo_6O_{10}(O-i-Pr)_{12}$ with pyridine.

Concluding Remarks. At the outset of this project, one of us had the idea that the addition of molecular oxygen to $Mo_2(OR)_6$ ($M \equiv M$) compounds would lead to a series of $Mo_2O_2(OR)_6$ ($M-M$) compounds. It is easy to envisage one of two structures for compounds of this formula where a d^1-d^1 interaction leads to a metal-metal single bond. These are shown in V and VI.



V



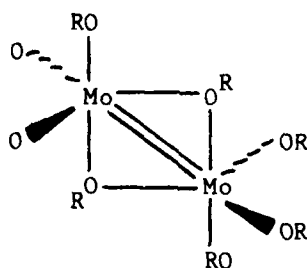
VI

In V, the Mo_2O_8 skeleton is formed by the fusing of two trigonal bipyramidal units which share a common equatorial-axial edge. This type of structure has been found in a number of molybdenum and tungsten compounds recently, including $[\text{Mo}(\text{NAr})(\mu\text{-NAr})(\text{OR})_2]_2$,⁴ $[\text{Mo}(\text{NO})(\text{OR})_2(\mu\text{-OR})]_2$ ⁴⁴ and $[\text{W}(\text{CMe})(\text{O-t-Bu})_2(\mu\text{-O-t-Bu})]_2$ ⁴⁵ which have no M-M bonds, $[\text{W}(\text{N}_2\text{CAR}_2)(\mu\text{-N}_2\text{CAR}_2)(\text{O-t-Bu})_2]$ ⁴⁶ which has a single W-W bond and in $\text{Mo}_2(\text{O-i-Pr})_8$ ¹² and $\text{Mo}_2(\mu\text{-S})_2(\text{S-t-Bu})_4(\text{HNMe}_2)_2$ ⁴⁷ which have double bonds. By defining the z axis to be coincident with the O-Mo-O axial ligands in V, and the x axis to be coincident with the Mo-O equatorial bridge, the d^1-d^1 metal-metal single bond would arise from interaction of $d_{xz}-d_{xz}$ Mo atomic orbitals.

In VI, which has two molybdenum atoms in a local square based pyramidal environment sharing a common basal edge, it is also easy to picture the formation of a M-M σ bond. By defining the z axis to be coincident with the apical Mo-oxo bond, the d_{xz} and d_{yz} Mo atomic orbitals will be used in Mo-O (oxo) π -bonding. One of the orbitals, d_{xy} or $d_{x^2-y^2}$, will be used in forming σ bonds to the RO ligands in the basal plane, and the other, which is not used in metal-ligand bonding, can form a M-M σ bond.

The reaction between $\text{Mo}_2(\text{OR})_6$ compounds and O_2 does not lead to the isolation of stable compounds of this formula, however. Whether this is

because of kinetic factors, that is to say a reactive intermediate $[\text{Mo}(\text{OR})_6\text{O}_2]^\dagger$ proceeds directly to $\text{O}_2\text{Mo}(\text{OR})_2$ and $\text{Mo}(\text{OR})_4$ by an asymmetric transition state, or because compounds of type V and VI are formed but are unstable with respect to asymmetric cleavage, is not known. It is certainly quite possible that a reactive intermediate $\text{Mo}_2(\text{OR})_6\text{O}_2$ could have the geometry shown in VII, from which oxo group formation and OR bridge cleavage could lead to $\text{O}_2\text{Mo}(\text{OR})_2$ and $\text{Mo}(\text{OR})_4$. Symmetrical intermediates of the type V and VI might never be formed in these reactions.



VII

We did attempt to prepare $[\text{MoO}(\text{OR})_3]_n$ compounds from the reaction between MoOCl_3 and LiOR (3 equiv), but without success. Only oily products were obtained, which still contained some chloride. No $\text{Mo}(\text{OR})_4$ or $\text{MoO}_2(\text{OR})_4$ compounds were detected. Regretably, this approach toward the synthesis of species of formula $\text{MoO}(\text{OR})_3$ was non-informative.

The new oxo-alkoxy compounds derived from the reactions between $\text{Mo}_2(\text{OR})_6$ compounds and molecular oxygen bear witness to the synthetic usefulness of M-M multiple bonds in preparing new mononuclear compounds.⁴⁸

EXPERIMENTAL SECTION

General procedures and the preparation of $\text{Mo}_2(\text{OR})_6$ compounds have been described.⁷ Methylene chloride was distilled from P_2O_5 under a nitrogen atmosphere. Pyridine was dried by storing over KOH for one week prior to distillation from barium oxide. tert-Butanol was distilled as an azeotrope with dry benzene and was stored over activated molecular sieves prior to use. iso-Propanol was distilled from sodium onto activated molecular sieves. A standard solution of neo-pentanol was prepared in toluene by dissolving a known quantity of the solid alcohol in toluene. Additional toluene was added to bring the volume of the solution to a known value, and the solution was stored over molecular sieves.

Analytical data and other spectroscopic and characterization data for the new compounds are reported in Tables I, II, III and IV.

^1H NMR spectra were recorded on a Varian Associates HR-220 NMR spectrometer in toluene- d^8 with a probe temperature of 16°C . Natural abundance ^{17}O NMR spectra were recorded on a Varian Associates XL-100 spectrometer in the Fourier transform mode. Infrared spectra were recorded on a Perkin-Elmer infrared spectrophotometer. Solid samples were prepared as Nujol mulls between CsI plates. Mass spectra were obtained by the method of direct insertion, courtesy of Mr. Peter Cook, Queen Mary College, London. Elemental analyses were performed by Analytische Laboratorien, Germany. Cryoscopic molecular weight determinations were done in benzene using a thermistor incorporated into a bridge circuit.

Reactions with Molecular Oxygen. All reactions between the metal alkoxides and oxygen were carried out in a similar manner. In the dry-box,

the metal complex was dissolved in a hydrocarbon solvent and placed in a round-bottomed flask containing a teflon covered magnetic stirring bar. The flask was fitted with an adapter containing a 2 mm stopcock. The flask was removed from the dry-box and attached to a double manifold vacuum line, consisting of a vacuum and dry molecular oxygen. The solution was frozen at -198°C (liquid nitrogen) and degassed by thawing in vacuo. The flask was refilled with dry oxygen. The solution was stirred under one atmosphere of oxygen (maintained by a mercury bubbler) until the reaction was complete.

Materials. Molecular oxygen was dried prior to use by passing the gas through a U-tube packed with activated molecular sieves. The U-tube was cooled to -78°C in a dry ice/acetone bath. iso-Propanol- d^6 was prepared by the reduction of acetone- d^6 with LiAlH_4 , followed by acid hydrolysis, extraction, and distillation. 99% Isotopic purity $^{18}\text{O}_2$ was obtained from Prochem Isotopes.

Preparations. $\text{MoO}_2(\text{O-t-Bu})_2$. $\text{Mo}_2(\text{O-t-Bu})_6$ (104 mg, 0.165 mmol) was dissolved in toluene (15 mL) in a 50 mL round-bottomed flask. The flask was filled with dry oxygen and the solution stirred for two h, during which time the color of the solution changed from orange to pale yellow. $\text{MoO}_2(\text{O-t-Bu})_2$ was obtained by stripping the solvent and vacuum distillation of the yellow liquid at 55°C , 10^{-4} torr. A cryoscopic molecular weight determination in benzene showed that $\text{MoO}_2(\text{O-t-Bu})_2$ is monomeric in solution, $M = 267 \pm 13$ (calculated for $\text{MoO}_2(\text{O-t-Bu})_2 = 274$). IR data: 320 m, 370 s, 463 s, 564 s, 587 s, 700 w, 799 s, 930 vs, 968 vs, 1025 s, 1087 m, 1160 vs, 1242 s and 1261 s cm^{-1} .

The average of two gas buret determinations confirmed the stoichiometry of 1, $O_2/Mo_2(O-t-Bu)_6 = 2.0 \pm 0.1$. When the reaction was done in a sealed NMR tube, a peak appeared at 1.09 ppm in addition to that of $MoO_2(O-t-Bu)_2$. Addition of tert-butanol enhanced the peak at 1.09 ppm. Vacuum distillation of the volatile components of this reaction to an NMR tube showed that tert-butanol is the only organic product. When the reaction was done using 1,4-cyclohexadiene as the solvent, tert-butanol and benzene were observed in the NMR spectrum in the ratio 2:1.

$MoO_2(O-t-Bu)_2(py)_2$. $MoO_2(O-t-Bu)_2$ (320 mg, 1.2 mmol) was dissolved in toluene (10 mL) under a nitrogen atmosphere. Pyridine (5.0 mL) was added to the flask with stirring. The solvent and excess pyridine were removed by stripping in vacuo. $MoO_2(O-t-Bu)_2(py)_2$ is a yellow liquid which loses pyridine when heated to $50^\circ C$ under vacuum. IR data: 315 s, 351 s, 428 w, 470 s, 610 s, 614 m, 620 w, 691 s, 750 s, 780 s, 920 s, 1030 m, 1068 m, 1160 s, 1210 w, 1230 m, 1570 m and 1594 m cm^{-1} .

$MoO_2(O-t-Bu)_2(bpy)$. $MoO_2(O-t-Bu)_2$ (220 mg, 0.80 mmol) was dissolved in toluene (25 mL) in a 50 mL round-bottomed flask fitted with a side arm addition tube. 2,2'-Bipyridine (126 mg, 0.80 mmol) was added to the solution via the addition tube with stirring. The solvent was stripped after stirring for 0.5 h, and the white solid was recrystallized from either toluene or methylene chloride. IR data: 321 s, 382 s, 412 w, 442 m, 467 w, 554 s, 622 w, 644 m, 721 m, 734 s, 750 w, 775 s, 795 w, 888 s, 901 m, 912 s, 935 s, 1021 s, 1055 w, 1098 w, 1150 w, 1172 s, 1221 m, 1253 m, 1310 m, 1575 m and 1595 s cm^{-1} .

MoO₂(O-i-Pr)₂, MoO₂(O-i-Pr)₂(py)₂, and MoO₂(O-i-Pr)₂(bpy). Mo₂(O-i-Pr)₆ (1.00 g, 1.83 mmol) was dissolved in toluene (25 mL) in a 100 mL round-bottomed flask under a nitrogen atmosphere. The solution was treated with dry molecular oxygen at 60°C for 24 h. During this time, the color of the solution changed from yellow to green to brown, and finally to pale yellow. MoO₂(O-i-Pr)₂ can be isolated as a white solid by reducing the volume of the solution to ca. 10 mL and adding pentane (25 mL). Cooling the solution causes precipitation of MoO₂(O-i-Pr)₂ as a white solid. Filtration and drying leads to decomposition. The stoichiometry of the overall reaction was determined by a gas buret experiment to be O₂/Mo₂(O-i-Pr)₆ = 2.0. When the reaction was done in a sealed vessel in toluene-d⁸ and the volatile components vacuum transferred to an NMR tube, iso-propanol and acetone were identified in the ¹H NMR spectrum. When Mo₂(O-i-Pr)₆ was treated with oxygen in 1,4-cyclohexadiene, iso-propanol and benzene were observed in the NMR spectrum in a 2:1 ratio, respectively.

MoO₂(O-i-Pr)₂ is not stable as a solid and decomposes to blue molybdenum oxides even when stored in sealed vials either under N₂ or in vacuo. It can, however, be kept in solution for several days before decomposition occurs. Several other methods for preparing MoO₂(O-i-Pr)₂ have been found, and are reported below.

MoO₂(O-i-Pr)₂: MoO₂(O-t-Bu)₂ + i-PrOH (excess). MoO₂(O-t-Bu)₂ (1.32 g, 4.82 mmol) was dissolved in toluene (25 mL) in a 100 mL round-bottomed flask under a nitrogen atmosphere. iso-Propanol (25 mL) was syringed into the solution while stirring. The solution volume was reduced to ca. 10 mL by stripping in vacuo. Solid MoO₂(O-i-Pr)₂ was isolated by adding pentane (25 mL), cooling, and filtering the white solid.

$\text{MoO}_2(\text{O-i-Pr})_2$: $\text{Mo}_6\text{O}_{10}(\text{O-i-Pr})_{12} + \text{O}_2 \cdot \text{Mo}_6\text{O}_{10}(\text{O-i-Pr})_{12}$ (200 mg, 0.138 mmol) was placed in a 25 mL round-bottomed flask under a nitrogen atmosphere. Toluene (10 mL) was added, and the solution treated with dry molecular oxygen. The solution was stirred at 60°C until all of the solid had dissolved, approximately 2.5 h. $\text{MoO}_2(\text{O-i-Pr})_2$ was isolated as a white solid by adding pentane (25 mL), cooling, and filtering.

$\text{MoO}_2(\text{O-i-Pr})_2$: $\text{Mo}_3\text{O}(\text{O-i-Pr})_{10} + \text{O}_2 \cdot \text{Mo}_3\text{O}(\text{O-i-Pr})_{10}$ (ca. 50 mg) was added to an NMR tube and dissolved in toluene- d^8 (0.20 mL). Dry molecular oxygen was added using a calibrated gas manifold and the tube was then sealed. The ^1H NMR spectrum was taken daily for three days, during which time the peaks corresponding to $\text{Mo}_3\text{O}(\text{O-i-Pr})_{10}$ declined and those for acetone, iso-propanol, and $\text{MoO}_2(\text{O-i-Pr})_2$ increased in intensity.

$\text{MoO}_2(\text{O-i-Pr})_2(\text{py})_2$. As an alternative to isolating the unstable solid $\text{MoO}_2(\text{O-i-Pr})_2$ in the above syntheses, the stable liquid $\text{MoO}_2(\text{O-i-Pr})_2(\text{py})_2$, can be isolated by adding pyridine to the flask after preparation. The solvent and excess pyridine are then removed by stripping in vacuo. $\text{MoO}_2(\text{O-i-Pr})_2(\text{py})_2$ is a yellow liquid which loses pyridine and begins to decompose when heated to 50°C in vacuo. IR data: 321 s, 455 s, 610 s, 690 s, 750 s, 794 s, 835 vs, 870 vs, 950 vs, 1031 s, 1064 s, 1100 s, 1155 s, 1212 s, 1322 s, 1480 s, 1575 w and 1601 s cm^{-1} .

$\text{MoO}_2(\text{O-i-Pr})_2(\text{bpy})$. $\text{MoO}_2(\text{O-i-Pr})_2$ (0.42 mmol) was prepared by treating $\text{MoO}_2(\text{O-t-Bu})_2$ (0.42 mmol) with $i\text{-PrOH}$ (excess) in a 50 mL round-bottomed flask fitted with a side arm addition tube under a nitrogen

atmosphere. 2,2'-Bipyridine (650 mg, 0.42 mmol) was added to the solution via an addition tube. After stirring for 30 min, the solvent was stripped in vacuo and the remaining white solid extracted with toluene (20 mL). The reaction volume was reduced and $\text{MoO}_2(\text{O-i-Pr})_2(\text{bpy})$ crystallized by cooling slowly to -10°C in a freezer. White crystals of $\text{MoO}_2(\text{O-i-Pr})_2(\text{bpy})$ were filtered and dried in vacuo. $\text{MoO}_2(\text{O-i-Pr})_2(\text{bpy})$ can also be recrystallized from methylene chloride. IR data: 316 s, 360 m, 420 m, 432 m, 552 w, 590 s, 523 w, 546 m, 718 w, 732 m, 779 s, 795 w, 835 w, 880 s, 899 s, 960 s, 1020 s, 1054 s, 1109 s, 1158 s, 1258 m, 1310 w, 1569 w and 1592 s cm^{-1} .

$\text{MoO}_2(\text{OCH}_2\text{-t-Bu})_2$. $\text{MoO}_2(\text{OCH}_2\text{-t-Bu})_2$ was prepared and isolated from $\text{Mo}_2(\text{OCH}_2\text{-t-Bu})_6$ in a procedure analogous to the preparation of $\text{MoO}_2(\text{O-i-Pr})_2$ from $\text{Mo}_2(\text{O-i-Pr})_6$ and oxygen. However, $\text{MoO}_2(\text{OCH}_2\text{-t-Bu})_2$ decomposes very rapidly when isolated as a solid. $\text{MoO}_2(\text{OCH}_2\text{-t-Bu})_2$ can be stabilized and isolated as an adduct with donor ligands such as pyridine and bpy.

Gas buret experiments confirmed the stoichiometry of the uptake of oxygen: $\text{O}_2/\text{Mo}_2(\text{OCH}_2\text{-t-Bu})_6 = 1.8$. When the reaction was done in a sealed vessel in toluene- d^8 and the volatile components vacuum transferred to an NMR tube, neo-pentanol was the only organic product identified. When $\text{Mo}_2(\text{OCH}_2\text{-t-Bu})_6$ was treated with oxygen in 1,4-cyclohexadiene, neo-pentanol and benzene were formed in the ratio of 2:1, respectively. Another method for the preparation of $\text{MoO}_2(\text{OCH}_2\text{-t-Bu})_2$ is reported below.

$\text{MoO}_2(\text{OCH}_2\text{-t-Bu})_2$: $\text{Mo}_3\text{O}(\text{OCH}_2\text{-t-Bu})_{10} + \text{O}_2$. $\text{Mo}_3\text{O}(\text{OCH}_2\text{-t-Bu})_{10}$ (ca. 50 mg) was added to an NMR tube and dissolved in toluene- d^8 (0.25 mL). Dry

molecular oxygen was added to the tube using a calibrated gas manifold and the tube was sealed. ^1H NMR spectra were recorded periodically over a four-week duration, during which time the peaks which corresponded to $\text{Mo}_3\text{O}(\text{OCH}_2\text{-t-Bu})_{10}$ decreased and those for neo-pentanol and $\text{MoO}_2(\text{OCH}_2\text{-t-Bu})_2$ increased in intensity. After five weeks, the contents of the tube had decomposed to blue molybdenum oxides.

$\text{MoO}_2(\text{OCH}_2\text{-t-Bu})_2(\text{py})_2$. $\text{MoO}_2(\text{O-t-Bu})_2$ (140 mg, 0.510 mmol) was prepared in toluene (10 mL) in a 50 mL round-bottomed flask from the reaction between $\text{Mo}_2(\text{O-t-Bu})_6$ (164 mg, 0.260 mmol) and molecular oxygen. 25 mL of a 1.66 M t-BuCH₂OH/toluene solution were added and the solvent was removed in vacuo until 2 mL of solution remained. Pyridine (10 mL) was syringed into the flask. The solvent and excess neo-pentanol were removed by stripping in vacuo. $\text{MoO}_2(\text{OCH}_2\text{-t-Bu})_2(\text{py})_2$ is a yellow liquid which loses pyridine when heated to 50°C under vacuum. IR data: 307 s, 360 s, 400 m, 459 s, 622 s, 642 m, 731 s, 769 s, 795 w, 890 s, 1018 s, 1040 m, 1052 s, 1098 m, 1145 m, 1175 w, 1220 w, 1249 m, 1285 w, 1313 s, 1570 w, 1590 s and 1601 m cm^{-1} .

$\text{MoO}_2(\text{OCH}_2\text{-t-Bu})_2(\text{bpy})$. $\text{MoO}_2(\text{O-t-Bu})_2$ (244 mg, 0.892 mmol) was prepared from $\text{Mo}_2(\text{O-t-Bu})_6$ (281 mg, 0.446 mmol) in toluene (10 mL) in a 50 mL round-bottomed flask fitted with a side arm addition tube. 30 mL of 1.66 M t-BuCH₂OH/toluene solution were added. The solvent was stripped in vacuo until about 2 mL remained. Toluene (15 mL) and 2,2'-bipyridyl (1.39 g, 0.892 mmol) were added. The solvent was stripped and the remaining white solid recrystallized from toluene. IR data: 305 s, 367 s, 401 m, 412 w,

461 s, 620 s, 644 m, 732 s, 770s, 795 w, 892 s, 918 s, 1018 s, 1044 m, 1058 s, 1088 w, 1148 m, 1170 w, 1220 w, 1252 m, 1287 w, 1313 s, 1570 w, 1592 s and 1600 m cm^{-1} .

MoO(O-t-Bu)₄. Mo(O-t-Bu)₄ (1.00 g, 2.58 mmol) was dissolved in toluene (10 mL) in a 50 mL round-bottomed flask under a nitrogen atmosphere. Oxygen was added to the flask and the solution stirred at room temperature, 1 Atmos, for 3 h. During this time, the color of the solution changed from green to yellow. The solvent was stripped to yield a thick yellow oil. MoO(O-t-Bu)₄ was obtained as a yellow liquid by vacuum distillation at 85°C (10⁻⁴ torr). IR data: 329 m, 365 s, 463 s, 562 s, 595 s, 691 w, 709 w, 741 w, 775 m, 790 m, 967 vs, 1020 m, 1090 w, 1160 s and 1235 s cm^{-1} .

MoO(O-i-Pr)₄. Mo₂(O-i-Pr)₈ (1.80 g, 2.71 mmol) was dissolved in toluene (25 mL) in a 50 mL round-bottomed flask under a nitrogen atmosphere. Oxygen was added to the flask and the solution stirred for 1 h, 1 Atmos (O₂). During this time, the color changed from blue to green to yellow. The solvent was stripped to yield a thick yellow oil. MoO(O-i-Pr)₄ was obtained as a yellow liquid by vacuum distillation at 60°C (10⁻⁴ torr). IR data: 325 m, 391 w, 465 m, 495 w, 601 s, 815 s, 840 s, 951 s, 1010 w, 1100 s, 1162 s, 1254 s, 1318 s, 1360 s, 1375 s, 1448 m and 1460 m cm^{-1} .

MoO(OCH₂-t-Bu)₄. [Mo(OCH₂-t-Bu)₄]_x (348 mg, 0.780 mmol) was dissolved in toluene (50 mL) in a 100 mL round-bottomed flask under a nitro-

gen atmosphere. Dry molecular oxygen was added to the flask. While stirring for 2 h under O_2 , 1 Atmos, at room temperature, the color changed from blue to green to yellow. The solvent was stripped to give a yellow solid. $MoO(OCH_2-t-Bu)_4$ was obtained by sublimation at $75-85^\circ C$, 10^{-4} torr, using a dry ice/acetone cooled probe. IR data: 300 w, 342 m, 399 m, 421 s, 509 s, 582 s, 619 s, 651 s, 683 s, 719 w, 749 m, 796 w, 915 s, 930 s, 990 s, 1018 s, 1035 s, 1212 m, 1260 m and 1290 w cm^{-1} .

$Mo_3O(O-i-Pr)_{10}$. $MoO(O-i-Pr)_4$ (640 mg, 1.84 mmol) was dissolved in toluene (25 mL) in a 50 mL round-bottomed flask fitted with a side arm addition tube under a nitrogen atmosphere. $Mo_2(O-i-Pr)_6$ (1.0 g, 1.84 mmol) was added via the side arm addition tube with stirring. The solution immediately turned from yellow to red and then to green. The solution was stirred for 1 h at room temperature and then the solvent was stripped. The green solid was recrystallized from methylene chloride. Green crystals of $Mo_3O(O-i-Pr)_{10}$ were filtered from the solution and dried in vacuo. IR data: 320 m, 460 w, 605 s, 818 m, 846 s, 930 s, 963 s, 1105 s, 1160 m, 1259 w, 1311 m and 1322 m cm^{-1} .

$Mo_3O(OCH_2-t-Bu)_{10}$. $MoO(OCH_2-t-Bu)_4$ (96 mg, 0.209 mmol) was dissolved in toluene (30 mL) in a 50 mL round-bottomed flask fitted with a side arm addition tube under a nitrogen atmosphere. $Mo_2(OCH_2-t-Bu)_6$ (149 mg, 0.209 mmol) was added via the side arm addition tube with stirring. The color of the solution immediately changed from yellow to green. The solution was stirred for 1.5 h at room temperature. The solvent was stripped in vacuo. The remaining green solids were recrystallized from hexane. Green crystals

of $\text{Mo}_3\text{O}(\text{OCH}_2\text{-t-Bu})_{10}$ were filtered from the solution and dried in vacuo. IR data: 354 w, 400 w, 465 w, 632 s, 655 m, 670 m, 715 w, 750 m, 795 m, 864 w, 928 w, 1012 s, 1039 s, 1210 s, 1055 s and 1290 m cm^{-1} .

$\text{Mo}_6\text{O}_{10}(\text{O-i-Pr})_{12}$: $\text{Mo}_2(\text{O-i-Pr})_6 + \text{O}_2 \cdot \text{Mo}_2(\text{O-i-Pr})_6$ (227 mg, 0.416 mmol) was dissolved in toluene (25 mL) in a 50 mL round-bottomed flask under a nitrogen atmosphere. The flask was filled with dry molecular oxygen and the solution stirred for 2 h at room temperature. During this time, the color of the solution changed from yellow to green. The solution was frozen at -198°C (liquid nitrogen) and the oxygen removed by thawing in vacuo. The flask was refilled with nitrogen and the solution stirred for one week at room temperature. Pentane (20 mL) was added to the flask and it was cooled to -10°C in a freezer. Yellow crystals of $\text{Mo}_6\text{O}_{10}(\text{O-i-Pr})_{12}$ precipitated overnight and were filtered and dried in vacuo. IR data: 395 m, 453 w, 473 m, 499 m, 555 w, 608 s, 642 m, 621 w, 640 w, 655 w, 822 s, 842 m, 850 m, 932 vs, 953 s, 986 s, 1099 s, 1118 s, 1170 w, 1260 w and 1319 m cm^{-1} .

$\text{Mo}_6\text{O}_{10}(\text{O-i-Pr})_{12}$: $\text{Mo}_2(\text{O-i-Pr})_8 + \text{MoO}_2(\text{O-i-Pr})_2 \cdot \text{MoO}_2(\text{O-i-Pr})_2$ (250 mg, 1.02 mmol) was prepared in toluene (30 mL) by alcoholysis of $\text{MoO}_2(\text{O-t-Bu})_2$ (279 mg, 1.02 mmol) in a 50 mL round-bottomed flask equipped with a side arm addition tube. $\text{Mo}_2(\text{O-i-Pr})_8$ (113 mg, 0.170 mmol) was added to the yellow solution. Upon mixing, the solution turned brown and yellow crystals of $\text{Mo}_6\text{O}_{10}(\text{O-i-Pr})_{12}$ began to precipitate. The flask was cooled to -10°C in a freezer. Yellow crystals of $\text{Mo}_6\text{O}_{10}(\text{O-i-Pr})_{12}$ were filtered and dried in vacuo.

$\text{Mo}_6\text{O}_{10}(\text{O-i-Pr})_{12}$: $\text{Mo}_3\text{O}(\text{O-i-Pr})_{10}$ + $\text{MoO}_2(\text{O-i-Pr})_2$. $\text{MoO}_2(\text{O-i-Pr})_2$ (177 mg, 0.720 mmol) was prepared in toluene (20 mL) by alcoholysis of $\text{MoO}_2(\text{O-t-Bu})_2$ (198 mg, 0.720 mmol) in a 50 mL round-bottomed flask equipped with a side arm addition tube. $\text{Mo}_3\text{O}(\text{O-i-Pr})_{10}$ (80 mg, 0.90 mmol) was added to the solution via the addition tube. The mixture was stirred for one week at 45°C, 1 Atmos (N_2), during which time the color changed from green to brown and yellow crystals began to form. The flask was placed in a freezer at -10°C. Yellow crystals of $\text{Mo}_6\text{O}_{10}(\text{O-i-Pr})_{12}$ formed overnight and were filtered and dried in vacuo.

$\text{Mo}_4\text{O}_8(\text{O-i-Pr})_4(\text{py})_4$: $\text{Mo}_2(\text{O-i-Pr})_6$ + O_2 + pyridine. $\text{Mo}_2(\text{O-i-Pr})_6$ (160 mg, 0.29 mmol) was dissolved in pyridine (20 mL) in a 50 mL round-bottomed flask under a nitrogen atmosphere. The flask was filled with molecular oxygen and the solution was allowed to stand at room temperature for 12 h, 1 Atmos (O_2). During this time, the solution changed from green to yellow and a small quantity of a red crystalline solid formed. The red solid was filtered and dried in vacuo. IR data: 320 m, 340 w, 394 w, 418 w, 431 m, 469 s, 501 w, 566 m, 597 s, 634 m, 653 s, 682 s, 722 s, 750 s, 810 m, 830 m, 914 s, 949 vs, 968 s, 1011 m, 1021 w, 1039 m, 1065 m, 1115 vs, 1154 m, 1212 s, 1312 m, 1572 m and 1601 s cm^{-1} .

$\text{Mo}_4\text{O}_8(\text{O-i-Pr})_4(\text{py})_4$: $\text{Mo}_6\text{O}_{10}(\text{O-i-Pr})_{12}$ + py (excess). $\text{Mo}_6\text{O}_{10}(\text{O-i-Pr})_{12}$ (50 mg, 0.034 mmol) was placed into a 10 mL round-bottomed flask under a nitrogen atmosphere. Pyridine (1.0 mL) was added to the flask. The yellow solid slowly dissolved to form a red solution. The flask was cooled slowly to -10°C. Red crystals of $\text{Mo}_4\text{O}_8(\text{O-i-Pr})_4(\text{py})_4$ formed overnight and were filtered and dried in vacuo.

X-Ray Structure Determinations. The diffractometers used in this study are upgraded versions of the instrument described in a previous work.⁴⁹ The new instrument eliminates the discrete logic circuitry previously used for the timer/scaler, shutter control, and meter drive functions, and instead uses a custom-built Z80 microcomputer with appropriate programmable interfaces. A serial interface allows bidirectional communication between the Z80 and the Texas Instruments TI980B minicomputer which is used for computing angular settings and overall control of the goniostat. Each TI980B is equipped with dual 8" floppy diskette drives for program and data storage, as well as several serial interfaces which are used for communication to other computers and peripheral devices in the laboratory network.

The Z80 software includes an automatic search routine which can be programmed to systematically examine a specified region of reciprocal space on the goniostat to locate diffraction maxima. Other Z80 software allows continuous plotting of the peak profile on a CRT terminal during data collection. Data collection can be performed at virtually any scan rate using normal θ - 2θ scans, omega scans, or fixed θ - 2θ modes. Complete details of the diffractometer interface and laboratory computer network will be published elsewhere.⁵⁰ The low temperature apparatus and data reduction techniques do not differ significantly from the earlier description.^{49,51}

Structure of $\text{MoO}_2(\text{O-i-Pr})_2(\text{bpy}) \cdot \frac{1}{2}\text{C}_7\text{H}_8$. A suitable crystal was transferred to the goniostat and cooled to -161°C . A systematic search of reciprocal space revealed no systematic absences as symmetry related

reflections, indicating a triclinic space group. Crystal and diffractometer data are summarized in Table XVII.

The structure was solved by a combination of direct methods and Fourier techniques. Two independent molecules were located in the asymmetric cell as well as disordered toluene solvent molecules. During the course of the refinement, one of the $\text{MoO}_2(\text{O-i-Pr})_2(\text{bpy})$ molecules was discovered to have a disordered O-i-Pr group, with three possible configurations for the methyl groups. Because of the disorder problems, no attempt was made to locate or refine hydrogen atoms. A final difference Fourier contained numerous peaks of intensity $0.3\text{--}0.9 \text{ e}/\text{\AA}^3$, many of which were unlikely positions for hydrogens. Anisotropic thermal parameters, a complete listing of distances and angles, and observed and calculated structure amplitudes are available as supplementary data.

Structure of $\text{Mo}_3\text{O}(\text{OCH}_2\text{-t-Bu})_{10} \cdot x\text{CH}_2\text{Cl}_2$. A suitable crystal was mounted as above and a systematic search revealed a set of maxima with orthorhombic symmetry and extinctions which could be indexed as Pbcn. Crystal and diffractometer data are given in Table XVII. The structure was solved by direct methods and Fourier techniques. A rather large percentage of the data (45%) were unobserved using the criteria $I_{\text{obs}} \geq 2.33\sigma(I_{\text{obs}})$. This was apparently due to a loss of a solvent molecule (CH_2Cl_2) and a disorder in one of the $\text{OCH}_2\text{-t-Bu}$ groups. While the disorder in the latter was clearly discernable in regular and difference Fourier maps, attempts to properly refine a disordered model led to unrealistic interatomic distances and angles. The partial occupancy solvent molecule was located in a difference Fourier after examination of the molecular packing⁵²

revealed a void of nearly 9 Å diameter in the structure. While the carbon atom of the solvent was not locatable, the two chlorine atoms refined to an average occupancy of 0.33. No attempt was made to locate hydrogen atoms and a final difference Fourier gave a nearly random distribution of peaks of intensity up to $0.7 \text{ e}/\text{Å}^3$. Anisotropic thermal parameters, complete listings of bonded distances and angles, and observed and calculated structure amplitudes are available as supplementary data.

Structure of $\text{Mo}_3\text{O}(\text{O-i-Pr})_{10}$. A suitable crystal was cooled to -162°C and a reciprocal lattice search revealed no systematic absences or symmetry, indicating a triclinic lattice. Crystal and diffractometer data are given in Table XVII. Two independent molecules were located by a combination of direct methods and Fourier techniques. Due to the number of atoms in the cell, the structure was refined in blocks during the full-matrix refinement. No attempt was made to locate or refine hydrogen atoms, although many were apparent in a final difference Fourier synthesis. A least squares fit⁵² of the molecular framework of the two independent molecules and the framework of the $\text{Mo}_3\text{O}(\text{OCH}_2\text{-t-Bu})_{10}$ molecule indicate the inner coordination geometry of the three are essentially identical. Anisotropic thermal parameters, complete listings of distances and angles, the molecular fit least squares, and observed and calculated structure amplitudes are available as supplementary data.

Structure of $\text{Mo}_6\text{O}_{10}(\text{O-i-Pr})_{12}$. A triclinic lattice was located in the diffraction maxima collected at -161°C . The structure was readily solved by a combination of Patterson and Fourier techniques. Crystal and

diffractometer data are given in Table XVII. Since there is only one molecule in the centrosymmetric space group, the molecule possesses crystallographic as well as molecular C_i symmetry. All hydrogen atoms were located in a difference Fourier phased on the non-hydrogen parameters and were allowed to vary isotropically for the final refinement. A final difference Fourier was featureless, with the largest peak being $0.5 \text{ e}/\text{\AA}^3$. Anisotropic thermal parameters, hydrogen coordinates, complete distances and angles, and a listing of observed and calculated structure amplitudes are available as supplementary data.

Acknowledgements. We thank the Office of Naval Research for support of this work. MHC is a recipient of a Henry and Camille Dreyfus Teacher-Scholar grant, 1979-84, and CCK is the Indiana University SOHIO Fellow, 1979-82.

Supplementary Data Available. Thermal parameters, hydrogen coordinates (for $\text{Mo}_6\text{O}_{10}(\text{O-i-Pr})_{12}$), complete distances and angles, least squares molecular fit analysis, and observed and calculated structure amplitudes for the single crystal structural studies (xxx pages). Ordering information is given on any current masthead page. Complete crystallographic data are also available, in microfiche form only, from the Indiana University Chemistry Library, Bloomington, Indiana 47405. Request MSC Report No. 81047 for $\text{MoO}_2(\text{O-i-Pr})_2(\text{bpy})$, No. 81006 for $\text{Mo}_3\text{O}(\text{OCH}_2\text{-t-Bu})_{10}$, No. 81029 for $\text{Mo}_3\text{O}(\text{O-i-Pr})_{10}$ and No. 81025 for $\text{Mo}_6\text{O}_{10}(\text{O-i-Pr})_{12}$ when ordering.

REFERENCES

1. Chisholm, M.H.; Huffman, J.C.; Ratermann, A.L. Inorg. Chem., submitted.
2. Chisholm, M.H.; Huffman, J.C.; Kirkpatrick, C.C. Inorg. Chem. 1981, 20, 871.
3. Chisholm, M.H.; Huffman, J.C.; Kirkpatrick, C.C. Inorg. Chem. 1983, 22, xxx.
4. Chisholm, M.H.; Folting, K.; Huffman, J.C.; Kirkpatrick, C.C.; Ratermann, A.R. J. Am. Chem. Soc. 1981, 103, 1305.
5. Chisholm, M.H.; Folting, K.; Huffman, J.C.; Kirkpatrick, C.C. J. Am. Chem. Soc. 1981, 103, 5397.
6. Chisholm, M.H.; Folting, K.; Huffman, J.C.; Kirkpatrick, C.C. J. Chem. Soc., Chem. Commun. 1982, 189.
7. Chisholm, M.H.; Cotton, F.A.; Murillo, C.A.; Reichert, W.W. Inorg. Chem. 1977, 16, 1801.
8. Chisholm, M.H.; Reichert, W.W.; Thornton, P. J. Am. Chem. Soc. 1978, 100, 2744.
9. Lever, A.P.B.; Wilshire, J.P.; Whan, S.K. Inorg. Chem. 1981, 20, 761.
10. Chin, D.H.; LaMar, G.N.; Balch, A.L. J. Am. Chem. Soc. 1980, 102, 5947.
11. Leddon, H.J.; Bonnet, M.; Galland, D. J. Am. Chem. Soc. 1981, 103, 6209.
12. Chisholm, M.H.; Cotton, F.A.; Extine, M.W.; Reichert, W.W. Inorg. Chem. 1978, 17, 2944.
13. Ashworth, T.V.; Chetcuti, M.J.; Farrugia, L.J.; Howard, J.A.K.; Jeffrey, J.C.; Mills, R.; Pain, G.N.; Stone, F.G.A.; Woodward, P. A.C.S. Symp. Ser. 1981, 155, Ch. 15.

14. Chen, G.J.-J.; McDonald, J.W.; Newton, W.E. Inorg. Chim. Acta 1979, 35, 93.
15. Templeton, J.L.; Bennett, C.W.; Chen, G.J.-J.; McDonald, J.W.; Newton, W.E. Inorg. Chem. 1981, 20, 1248.
16. Chisholm, M.H.; Huffman, J.C.; Leonelli, J.; Rothwell, I.P. J. Am. Chem. Soc. 1982, 104, 7030.
17. Chisholm, M.H.; Folting, K.; Huffman, J.C.; Rothwell, I.P. J. Am. Chem. Soc. 1982, 104, 4389.
18. Chisholm, M.H.; Cotton, F.A.; Extine, M.W.; Kelly, R.L. J. Am. Chem. Soc. 1979, 101, 7645.
19. Klemperer, W.G. Angew. Chem., Int. Ed. Engl. 1978, 17, 246.
20. Kidd, R.G. Can. J. Chem. 1967, 45, 605.
21. Freeman, M.A.; Schultz, F.A.; Reilley, C.N. Inorg. Chem. 1982, 21, 567.
22. Miller, K.F.; Wentworth, R.A.D. Inorg. Chem. 1979, 18, 984.
23. Haymore, B.L.; Nugent, W.A. Coord. Chem. Rev. 1980, 31, 123.
24. Chisholm, M.H. Polyhedron 1983, 2, xxx.
25. Appleton, T.G.; Clark, H.C.; Manzer, L.M. Coord. Chem. Rev. 1973, 10, 335.
26. Chisholm, M.H.; Huffman, J.C.; Rothwell, I.P.; Woodruff, W.H.; Bradley, P.G.; Kress, N. J. Am. Chem. Soc. 1981, 103, 4945.
27. Bradley, D.C.; Mehrotra, R.C.; Gaur, D.P. "Metal Alkoxides", Academic Press: New York, 1978.
28. Johnson, D.A.; Taylor, J.C.; Waugh, A.B. J. Inorg. Nucl. Chem. 1980, 42, 1271.
29. Oliver, I.G.; Worrall, I.J. J. Chem. Soc. A 1970, 2347.

30. Alyea, E.C.; Basi, J.S.; Bradley, D.C.; Chisholm, M.H. J. Chem. Soc. A 1971, 772.
31. Bradley, D.C.; Chisholm, M.H.; Extine, M.W.; Stager, M.E. Inorg. Chem. 1977, 16, 179.
32. Muller, A.; Jostes, R.; Cotton, F.A. Angew. Chem., Int. Ed. Engl. 1980, 19, 875.
33. Bino, A.; Cotton, F.A.; Dori, Z. J. Am. Chem. Soc. 1978, 100, 5252.
34. Bino, A.; Cotton, F.A.; Dori, Z. J. Am. Chem. Soc. 1981, 103, 243.
35. McCarroll, W.H.; Katz, L.; Ward, J. J. Am. Chem. Soc. 1957, 79, 5410.
36. Ansell, G.B.; Katz, L. Acta Crystallogr. 1966, 21, 482.
37. McCarley, R.E.; Torardi, C.C. J. Solid State Chem. 1981, 7, 393.
38. Chisholm, M.H.; Cotton, F.A.; Extine, M.W.; Reichert, W.W. J. Am. Chem. Soc. 1978, 100, 1727.
39. Chisholm, M.H.; Folting, K.; Huffman, J.C.; Kirkpatrick, C.C.; Leonelli, J. J. Am. Chem. Soc. 1982, 103, 6093.
40. Colton, R.; McCormick, M.J. Coord. Chem. Rev. 1980, 31, 1.
41. Cotton, F.A.; Troup, J.M. J. Am. Chem. Soc. 1974, 96, 1233.
42. Cotton, F.A.; Frenz, B.A.; Kruczynski, L. J. Am. Chem. Soc. 1973, 95, 951.
43. Bailey, W.I., Jr.; Chisholm, M.H.; Cotton, F.A.; Rankel, L. J. Am. Chem. Soc. 1978, 100, 5764.
44. Chisholm, M.H.; Cotton, F.A.; Extine, M.W.; Kelly, R.L. J. Am. Chem. Soc. 1978, 100, 3354.
45. Chisholm, M.H.; Hoffman, D.M.; Huffman, J.C. Inorg. Chem. in press.
46. Chisholm, M.H.; Huffman, J.C.; Ratermann, A.R. results to be published.
47. Chisholm, M.H.; Corning, J.C.; Huffman, J.C. Inorg. Chem. 1982, 21, 286.

48. Walton, R.A. A.C.S. Symp. Ser. 1981, 155, 207.
49. Huffman, J.C.; Lewis, L.N.; Caulton, K.G. Inorg. Chem. 1980, 19, 2755.
50. Huffman, J.C., Ph.D. Thesis, Indiana University, Bloomington, Indiana, 1974.
51. Huffman, J.C.; Streib, W.E.; Sporleder, C.R. in preparation.
52. Nyburg, S.C. J. Appl. Cryst. 1979, 117.
53. Ardon, M.; Cotton, F.A.; Dori, Z.; Fang, A.; Kapon, M.; Reisner, G.M.; Shaia, M. J. Am. Chem. Soc. 1982, 104, 5394.
54. Cotton, F.A.; Morehouse, S.M. Inorg. Chem. 1965, 4, 1377.
55. Knox, J.R.; Prout, C.K. Acta Cryst. 1969, 25B, 1857.
56. Drew, M.G.B.; Kay, A. J. Chem. Soc. (A) 1971, 1846.

CAPTIONS TO FIGURES

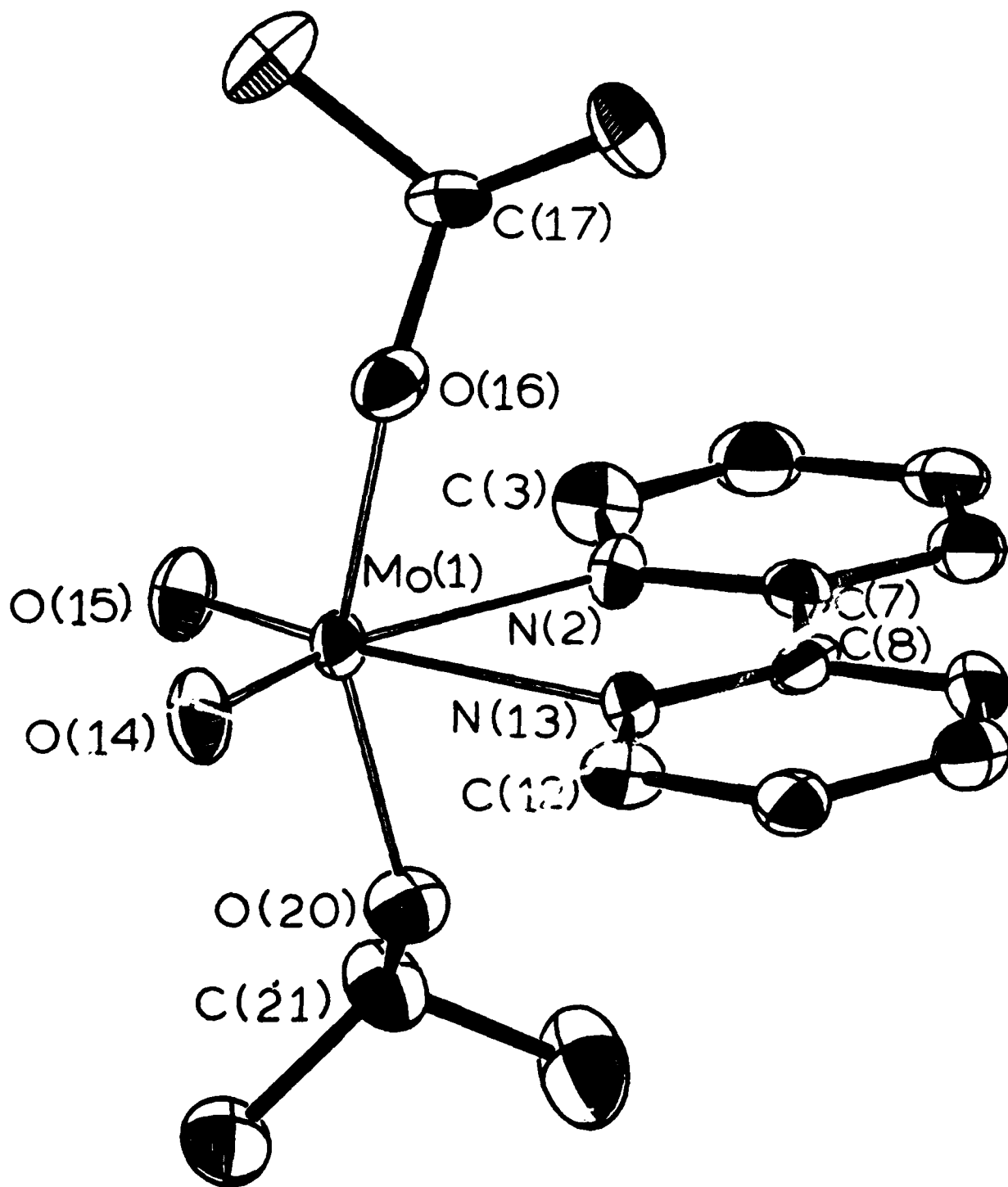
Figure 1. An ORTEP view of the $\text{MoO}_2(\text{O-i-Pr})_2(\text{bpy})$ molecule giving the atom number scheme used in the tables.

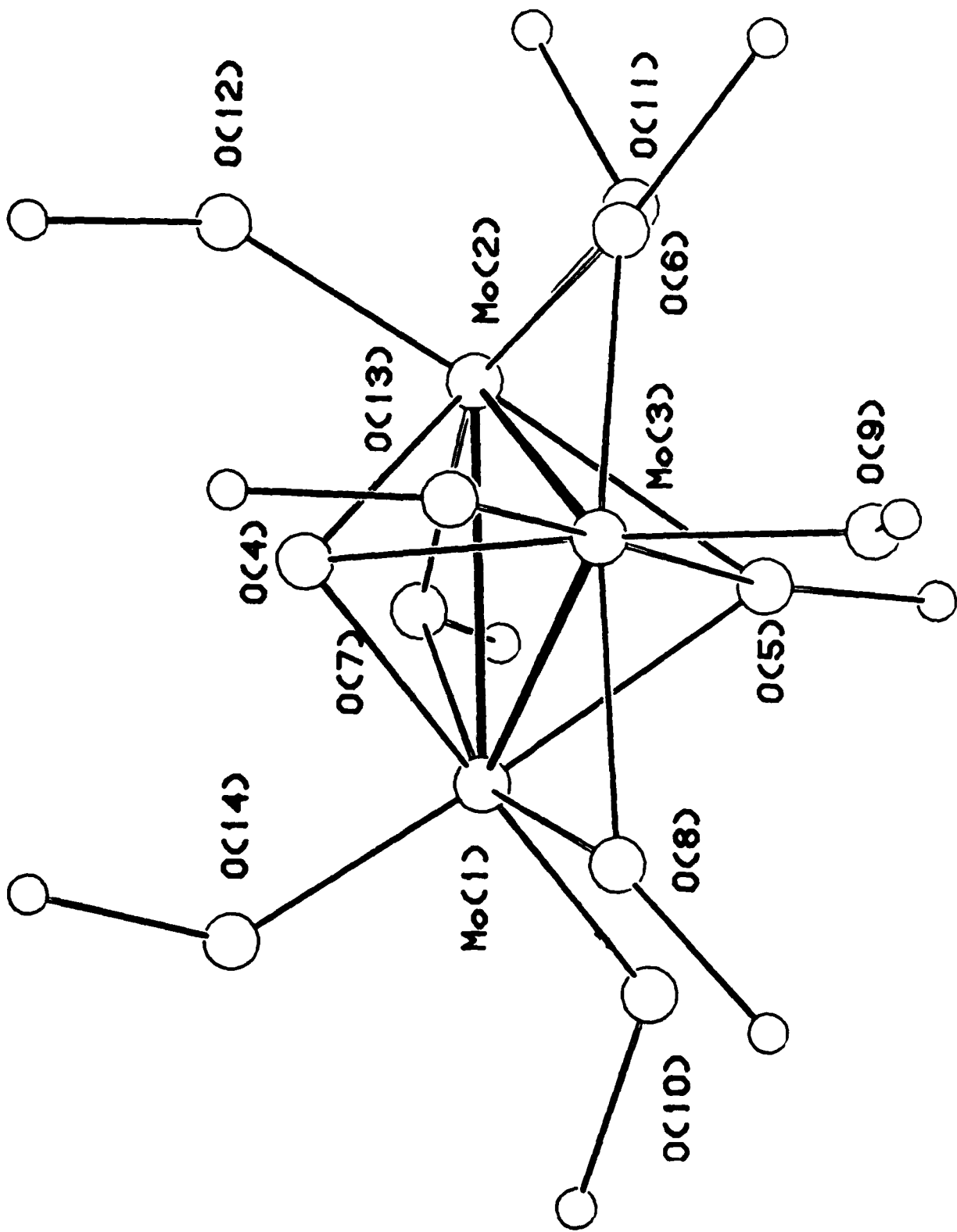
Figure 2. An ORTEP view of the central Mo_3O_{11} skeleton found in the $\text{Mo}_3\text{O}(\text{OR})_{10}$ molecules ($\text{R} = \text{CH}_2\text{-t-Bu}$ and i-Pr) showing the atom number scheme used in the tables. The oxo ligand is O(4).

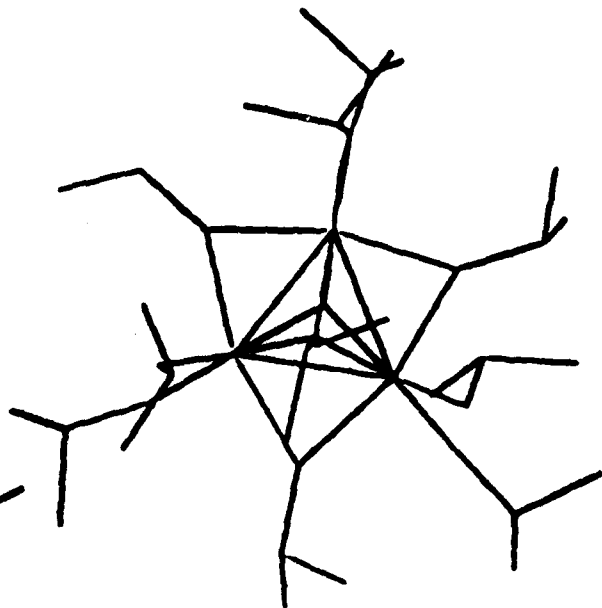
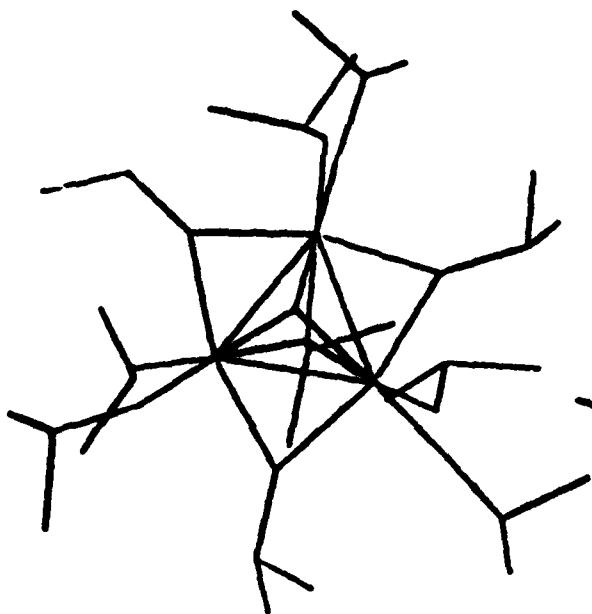
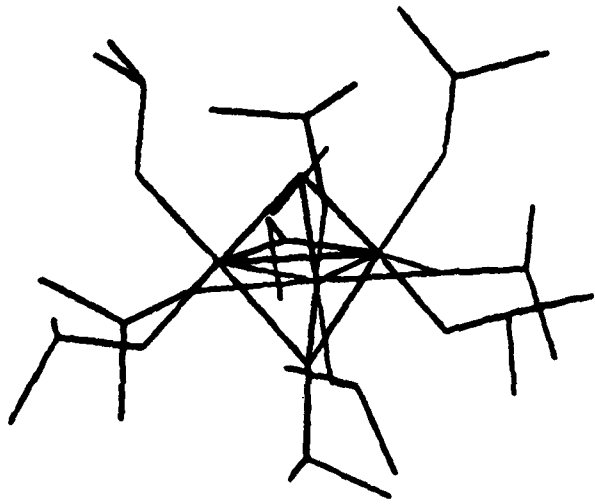
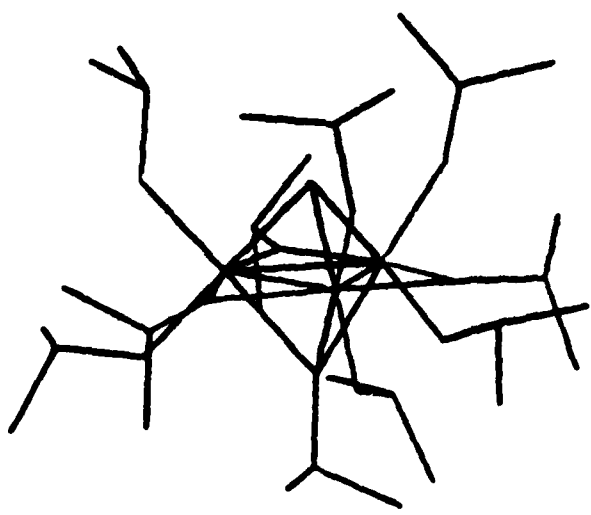
Figure 3. Two stereo views of one of the two $\text{Mo}_3\text{O}(\text{O-i-Pr})_{10}$ molecules found in the asymmetric unit of the unit cell.

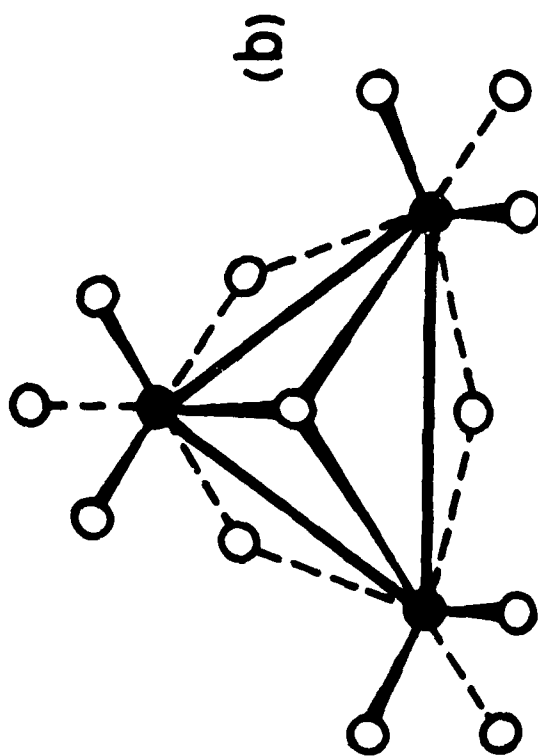
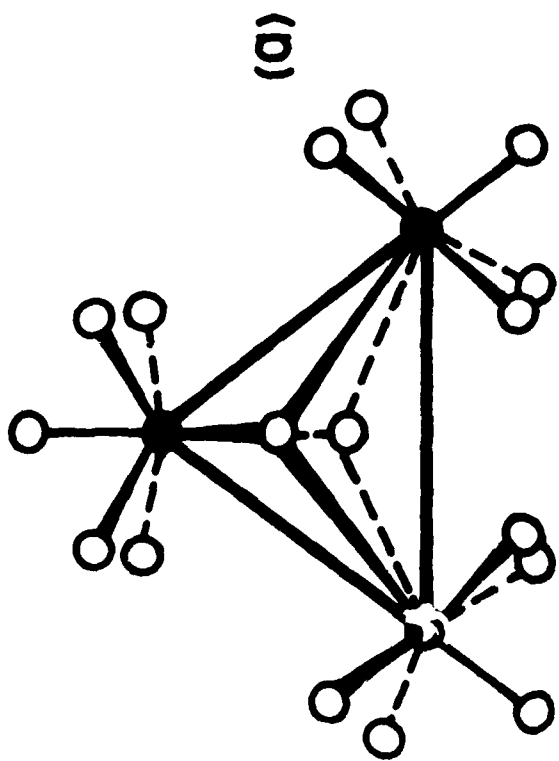
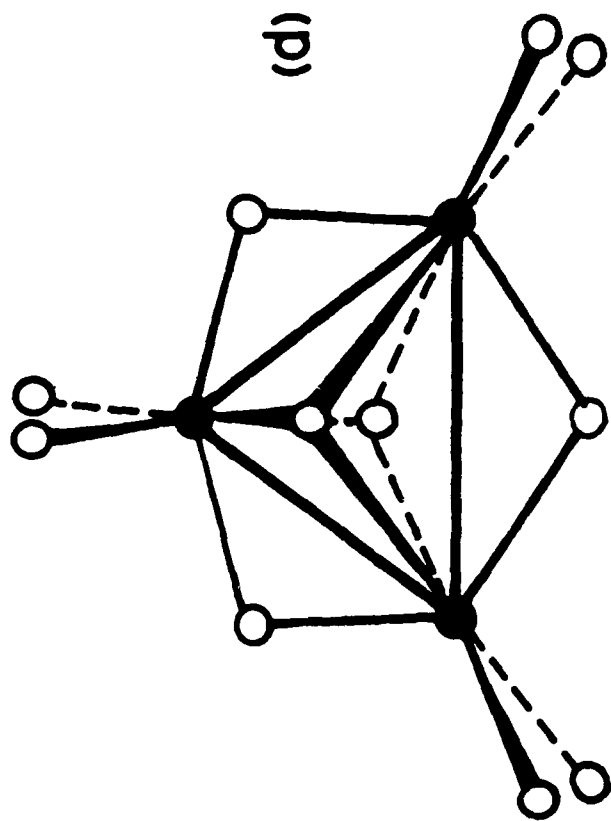
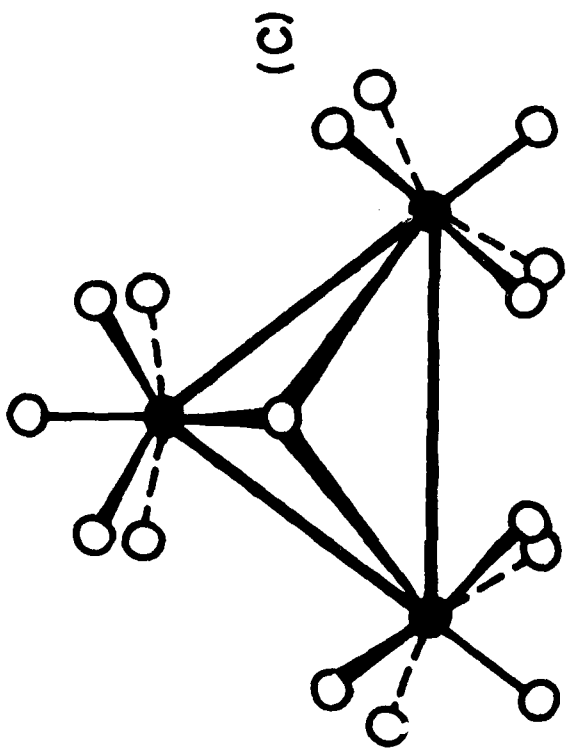
Figure 4. Prototypal representations of the four types of trinuclear cluster structures known for molybdenum and/or tungsten compounds.⁵³ (a) The bicapped structure found in $[\text{M}_3\text{X}_3(\text{O}_2\text{CR})_6(\text{H}_2\text{O})_3]^{n-}$ species. (b) The trigonal M_3O_4 type found in, for example, the $\text{Mo}(\text{IV})$ aquo ion. (c) The hemicapped structure found in $[\text{W}_3\text{O}(\text{O}_2\text{CMe})_6(\text{H}_2\text{O})_3]\text{ZnBr}_4 \cdot 8\text{H}_2\text{O}$. (d) The structure found in $\text{Mo}_3\text{O}(\text{OR})_{10}$ compounds reported here.

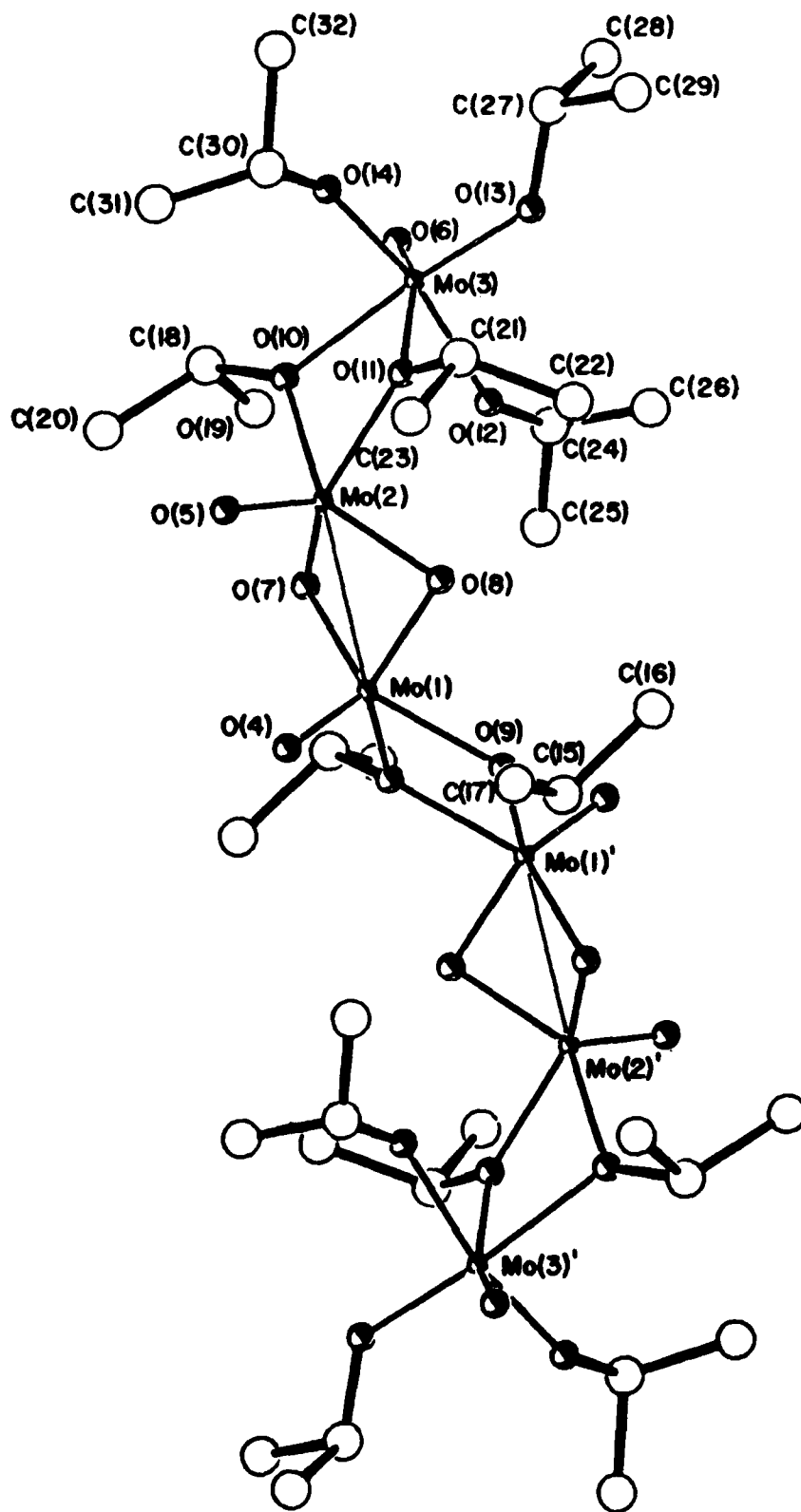
Figure 5. View of the centrosymmetric $\text{Mo}_6\text{O}_{10}(\text{O-i-Pr})_{10}$ molecule giving the atom number scheme used in the tables.



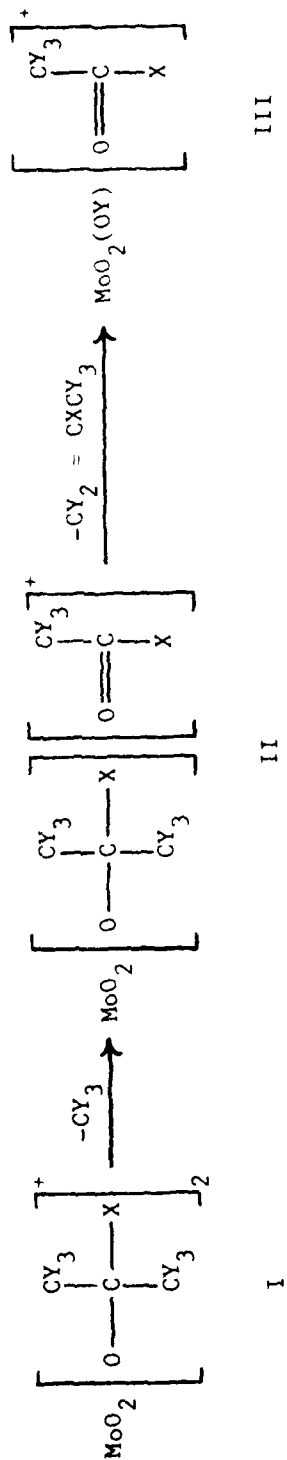








SCHEME 1



Compound	X	Y	I ^a	m/e	III
MoO ₂ (O-t-Bu) ₂	Me	H	276	261	205
MoO ₂ (O-i-Pr) ₂ (bpy)	H	H	248	233	191
Mo ¹⁸ O ₂ (O-i-Pr) ₂ (bpy)	H	H	252	237	195
MoO ₂ (O-i-Pr-d ⁶) ₂ (bpy)	H	D	260	242	195

^aNo molecular ions are observed in the mass spectrum. All ions are based on ⁹⁸Mo.

Table I. Physical Characteristics of Oxy-Alkoxy-Molybdenum Compounds.

Compound	Physical State, 25°C	Color	Volatility ^a	Molecular Weight ^b
MoO ₂ (O-t-Bu) ₂	liquid	yellow	55°C	267±13(274)
MoO ₂ (O-t-Bu) ₂ (bpy)	solid	white	d	
MoO ₂ (O-i-Pr) ₂ (bpy)	solid	white	d	
MoO ₂ (OCH ₂ -t-Bu) ₂ (bpy)	solid	white	d	
MoO(O-t-Bu) ₄	liquid	yellow	85°C	
MoO(O-i-Pr) ₄	liquid	yellow	60°C	410±30(348)
MoO(OCH ₂ -t-Bu) ₄	solid	yellow	70°C	499±50(460)
Mo ₃ O(O-i-Pr) ₁₀	solid	green	d	
Mo ₃ O(OCH ₂ -tBu) ₁₀	solid	green	d	
Mo ₆ O ₁₀ (O-i-Pr) ₁₂	solid	yellow	d	483±50(1444)
Mo ₄ O ₈ (O-i-Pr) ₄ (py) ₄ ·2py	solid	red	d	

^aBoiling point at 10⁻⁴ torr for liquids. Sublimation temperature for solids at 10⁻⁴ torr. d = decomposes. ^bCryoscopic determination in benzene: Found (Calcd based on formula).

Table II. Analytical Data for Oxy-Alkoxy-Molybdenum Compounds.

Compound	%C	Found %H	%N	Calculated %H	%N
$\text{MoO}_2(\text{O}-t\text{-Bu})_2$	35.45	6.98	6.67	6.62	6.51
$\text{MoO}_2(\text{O}-t\text{-Bu})_2(\text{bpy})$	50.03	5.93	7.09	6.09	6.51
$\text{MoO}_2(\text{O}-i\text{-Pr})_2(\text{bpy})$	47.79	5.34	7.09	5.51	6.96
$\text{MoO}_2(\text{OCH}_2-t\text{-Bu})_2(\text{bpy})$	52.14	6.73	6.03	6.60	6.11
$\text{MoO}(\text{O}-t\text{-Bu})_4$	47.33	8.81		8.97	
$\text{MoO}(\text{O}-i\text{-Pr})_4$	41.11	7.90		8.10	
$\text{MoO}(\text{OCH}_2-t\text{-Bu})_4$	51.84	9.42		9.63	
$\text{Mo}_3\text{O}(\text{O}-i\text{-Pr})_{10}$	40.17	7.71		7.89	
$\text{Mo}_3\text{O}(\text{OCH}_2-t\text{-Bu})_{10}$	50.83	9.17		9.43	
$\text{Mo}_6\text{O}_{10}(\text{O}-i\text{-Pr})_{12}$	29.52	5.66		5.86	
$\text{Mo}_4\text{O}_8(\text{O}-i\text{-Pr})_4(\text{py})_4 \cdot 2\text{py}$	41.17	4.83	6.71	5.00	6.61

Table III. ^{17}O and ^1H NMR Data for Oxy-Alkoxy-Molybdenum Compounds.

Compound	$\delta^{17}\text{O}$ ($\Delta\gamma$) ^a	$\delta^1\text{H}$ ^b
$\text{MoO}_2(\text{O}-t\text{-Bu})_2$	862(90)	1.20
$\text{MoO}_2(\text{O}-t\text{-Bu})_2(\text{py})_2$	885(119)	8.50 (m, 2H); 6.99 (m, 1H); 6.68 (m, 2H); 1.02 (s, 9H)
$\text{MoO}_2(\text{O}-t\text{-Bu})_2(\text{bpy})$		8.55 (m, 1H); 7.22 (m, 1H); 7.12 (m, 1H); 6.69 (m, 1H); 1.18 (s, 9H)
$\text{MoO}_2(\text{O}-i\text{-Pr})_2(\text{py})_2$	878(32)	8.53 (m, 2H); 6.99 (m, 1H); 6.68 (m, 2H); 4.77 (sept, 1H); 1.30 (d, 6H)
$\text{MoO}_2(\text{O}-i\text{-Pr})_2(\text{bpy})$		8.52 (m, 1H); 7.20 (m, 1H); 7.10 (m, 1H); 6.66 (m, 1H); 4.63 (sept, 1H); 1.02 (d, 6H)
$\text{MoO}_2(\text{OCH}_2-t\text{-Bu})_2(\text{py})_2$	872(330)	8.53 (m, 2H); 6.99 (m, 1H); 6.65 (m, 2H); 3.80 (s, 2H); 0.60 (s, 9H)
$\text{MoO}_2(\text{OCH}_2-t\text{-Bu})_2(\text{bpy})$		8.49 (m, 1H); 7.18 (m, 1H); 7.12 (m, 1H); 6.99 (m, 1H); 3.86 (s, 2H); 0.68 (s, 9H)
$\text{MoO}(\text{O}-t\text{-Bu})_4$	970(224)	1.45

Table III. Continued.

Compound	$\delta^{17}\text{O}$ ($\Delta\gamma$) ^a	$\delta^{1}\text{H}$ ^b
$\text{MoO}(\text{O}-i\text{-Pr})_4$	894(150)	4.77 (sept, 1H); 1.34 (d, 6H)
$\text{MoO}(\text{OCH}_2\text{-t-Bu})_4$		4.54 (s, 2H); 1.04 (s, 9H)
$\text{Mo}_3\text{O}(\text{O}-i\text{-Pr})_{10}$		5.67 (sept, 2H); 5.42 (sept, 3H); 4.64 (sept, 3H); 4.00 (sept, 1H); 1.64 (d, 18H); 1.57 (s, 18H); 1.19 (sept, 6H); 1.16 (s, 18H)
$\text{Mo}_3\text{O}(\text{OCH}_2\text{-t-Bu})_{10}$		4.87 (s, 6H); 4.76 (s, 6H); 4.14 (s, 6H); 3.84 (s, 2H); 1.02 (s, 27H); 1.13 (s, 27H); .999 (s, 27H); .931 (s, 9H)
$\text{Mo}_6\text{O}_{10}(\text{O}-i\text{-Pr})_{12}$		5.18; 3.54; 1.50; 1.16 (all broad) 75°C: 4.30 (sept, 1H); 1.30 (d, 6H)

^aChemical shifts are in ppm downfield from H_2^{17}O . All peak widths at half height are given in Hz. Spectra recorded at 35°C in toluene. No signals were observed for alkoxide oxygens. ^bChemical shifts are in ppm downfield from TMS. Parenthetical values give peak multiplicity, followed by relative proton integration. All spectra are recorded in toluene-d⁸ at 16°C, unless otherwise stated. s = singlet, d = doublet, sept = septet, m = multiplet.

Table IV. Terminal Molybdenum-Oxygen Stretching Frequencies for
Oxy-Alkoxy-Molybdenum Compounds.

Compound	$\gamma(\text{Mo}-^{16}\text{O}) \text{ cm}^{-1}$	$\gamma(\text{Mo}-^{18}\text{O}) \text{ cm}^{-1}$
$\text{MoO}_2(\text{O}-t\text{-Bu})_2^{\text{a}}$	968, 930	920, 887
$\text{MoO}_2(\text{O}-t\text{-Bu})_2(\text{bpy})^{\text{b}}$	912, 888	863, 843
$\text{MoO}_2(\text{O}-i\text{-Pr})_2(\text{bpy})^{\text{b}}$	899, 880	
$\text{MoO}_2(\text{OCH}_2-t\text{-Bu})_2(\text{bpy})^{\text{b}}$	918, 893	872, 851
$\text{MoO}(\text{O}-t\text{-Bu})_4^{\text{a}}$	967	
$\text{MoO}(\text{O}-i\text{-Pr})_4^{\text{a}}$	951	
$\text{MoO}(\text{OCH}_2-t\text{-Bu})_4^{\text{b}}$	915	
$\text{Mo}_4\text{O}_8(\text{O}-i\text{-Pr})_4(\text{py})_4^{\text{b}}$	951, 918	904, 873

^aTaken as a neat liquid between CsI plates. ^bTaken as a Nujol mull between CsI plates.

Table V. Fractional Coordinates for the $\text{MoO}_2(\text{O-i-Pr})_2(\text{bpy})_2$

Molecule.

Atom	10^4 x	10^4 y	10^4 z
Mo(1)	5167(1)	8152(1)	3020.7(5)
N(2)	5882(6)	10221(10)	2537(4)
C(3)	5296(8)	11319(13)	2419(6)
C(4)	5694(8)	12545(14)	2142(6)
C(5)	6747(8)	12696(12)	2005(5)
C(6)	7372(8)	11527(12)	2133(5)
C(7)	6886(7)	10352(11)	2409(5)
C(8)	7474(7)	9084(12)	2559(5)
C(9)	8502(7)	9073(12)	2464(6)
C(10)	8991(7)	7865(13)	2635(6)
C(11)	8437(8)	6675(13)	2860(5)
C(12)	7398(7)	6774(12)	2944(5)
N(13)	6934(6)	7959(9)	2804(4)
O(14)	5068(5)	6524(9)	3333(4)
O(15)	3989(5)	8743(9)	2999(4)
O(16)	5132(5)	9921(8)	3957(3)
C(17)	4922(8)	11723(12)	4332(6)
C(18)	3938(8)	12138(14)	5051(6)
C(19)	5833(9)	12356(15)	4563(7)
O(20)	5743(5)	6725(8)	1935(4)
C(21)	5392(9)	6747(14)	1338(6)
C(22)	4960(9)	5106(14)	1053(6)
C(23)	6286(11)	6959(18)	709(7)
Mo(1)'	743(1)	2019(1)	2208.2(5)
N(2)'	1388(5)	4351(9)	1947(4)
C(3)'	1138(7)	4851(12)	1445(5)
C(4)'	1475(7)	6311(12)	1319(5)
C(5)'	2066(7)	7260(12)	1707(5)
C(6)'	2340(7)	6725(12)	2227(5)
C(7)'	1991(6)	5264(11)	2327(5)
C(8)'	2252(7)	4564(11)	2834(5)
C(9)'	2900(7)	5315(13)	3231(6)
C(10)'	3141(7)	4542(13)	3688(5)
C(11)'	2722(7)	3065(13)	3719(6)
C(12)'	2108(7)	2387(13)	3300(6)
N(13)'	1861(6)	3128(9)	2868(4)
O(14)'	512(5)	557(8)	2624(4)
O(15)'	9(5)	1765(8)	1634(4)
O(16)'	-155(5)	3935(8)	3083(3)
C(17)'	-552(7)	4069(12)	3875(5)
C(18)'	-420(9)	5844(13)	4383(6)
C(19)'	-1663(8)	3771(14)	4050(6)
O(20)'	2047(5)	823(8)	1438(3)

Table V. Continued.

Atom	10^4 x	10^4 y	10^4 z
C(21)'	2662(11)	789(16)	715(8)
C(22)'	3742(40)	926(67)	720(28)
C(23)'	2371(35)	9014(54)	141(25)
C(22A)'	3862(32)	945(54)	989(22)
C(23A)'	3645(25)	152(42)	423(19)
C(22B)'	2956(28)	-697(43)	135(19)
C(23B)'	2082(30)	-540(49)	104(23)
C(1)''	343(9)	-139(15)	4346(7)
C(2)''	1490(12)	-607(19)	4995(9)
C(3)''	445(18)	-262(31)	5030(14)
C(4)''	1361(18)	-530(29)	4307(13)
C(5)''	-581(21)	215(33)	4371(15)
C(6)''	9512(24)	6916(39)	295(17)
C(7)''	8829(22)	5561(36)	730(15)
C(8)''	10755(20)	6242(34)	-501(15)
C(9)''	9275(21)	8189(37)	352(15)
C(10)''	716(23)	3863(45)	-445(17)
C(11)''	6(27)	6486(42)	-52(19)
C(12)''	9391(22)	4883(42)	406(16)

Table VI. Selected Bond Distances (Å) for the $\text{MoO}_2(\text{O}-i\text{-Pr})_2$ (bpy) Molecule.

Bond	Distance (Å)	Bond	Distance (Å)
Mo(1)-O(14)	1.689(7)	O(20)-C(21)	1.432(11)
Mo(1)-O(15)	1.723(6)	N(2)-C(3)	1.352(12)
Mo(1)-O(16)	1.914(6)	N(2)-C(7)	1.350(12)
Mo(1)-O(20)	1.945(6)	N(13)-C(8)	1.351(12)
Mo(1)-N(2)	2.367(8)	N(13)-C(12)	1.336(11)
Mo(1)-N(13)	2.346(8)	C-C in bpy ring	1.40(1) average
O(16)-C(17)	1.405(11)	C-C in iso-propyl	1.53(1) average

Table VII. Selected Bond Angles for the $\text{MoO}_2(\text{O}-i\text{-Pr})_2$ (bpy) Molecule.

Bond	Angle ($^\circ$)	Bond	Angle ($^\circ$)
O(14)-Mo(1)-O(15)	108.0(3)	O(16)-Mo(1)-N(2)	81.0(3)
O(14)-Mo(1)-O(16)	96.6(3)	O(16)-Mo(1)-N(13)	81.0(3)
O(14)-Mo(1)-O(20)	96.7(3)	O(20)-Mo(1)-N(2)	79.9(3)
O(14)-Mo(1)-N(2)	160.9(3)	O(20)-Mo(1)-N(13)	78.3(3)
O(14)-Mo(1)-N(13)	91.7(3)	N(2)-Mo(1)-N(13)	69.2(3)
O(15)-Mo(1)-O(16)	100.4(3)	Mo(1)-O(16)-C(17)	140.0(6)
O(15)-Mo(1)-O(20)	94.7(3)	Mo(1)-O(20)-C(21)	128.2(6)
O(15)-Mo(1)-N(2)	91.0(3)	Mo-O-Ca in iso-propoxide	130.0(10) average
O(15)-Mo(1)-N(13)	159.8(3)	C8-Ca-C8 in iso-propoxide	109.0(10) average
O(16)-Mo(1)-O(20)	155.7(3)	C-C-C in bpy ring	120.0(10) average

Table VIII. Significant Ions in the Mass Spectrum of the New Oxy-Alkoxy Compounds.

Compound	Temp (°C)	m/e ^a
MoO ₂ (O-t-Bu) ₂	56	211(22); 205(100)
MoO ₂ (O-t-Bu) ₂ (bpy)	69	261(100); 205(20)
MoO ₂ (O-i-Pr) ₂ (bpy)	74	233(71); 191(100)
Mo ¹⁸ O ₂ (O-i-Pr) ₂ (bpy)	60	237(100); 195(7.7)
MoO ₂ (O-i-Pr-d ⁶) ₂ (bpy) ^b	102	242(73); 195(100)
MoO ₂ (OCH ₂ -t-Bu) ₂ (bpy)	75	274(53); 256(100)
MoO(O-t-Bu) ₄	45	333(10); 277(5.1); 221(100); 165(80)
MoO(O-i-Pr) ₄	58	291(14); 249(9.3); 207(47); 165(100)
MoO(OCH ₂ -t-Bu) ₄	7	375(100)

^a All ions are based on ⁹⁸Mo. Parenthetical value is the relative percent intensity. Base peak 100%.

^b (O-i-Pr-d⁶) represents [OCH(CD₃)₂].

Table IX. Fractional Coordinates for the $\text{Mo}_3\text{O}(\text{OCH}_2\text{-t-Bu})_{10}$
Molecule.

Atom	10^4 x	10^4 y	10^4 z
Mo(1)	5952(1)	2582(2)	153(2)
Mo(2)	6247(1)	2604(2)	-1033(2)
Mo(3)	6373(1)	1580(2)	-220(2)
O(4)	6509(7)	2609(15)	-95(12)
O(5)	5807(9)	1849(16)	-654(17)
O(6)	6496(7)	1667(14)	-1240(12)
O(7)	5876(8)	3261(14)	-643(14)
O(8)	6048(9)	1659(16)	646(14)
O(9)	6264(8)	568(14)	-271(13)
O(10)	5425(7)	2551(16)	390(12)
O(11)	6007(7)	2602(17)	-1930(11)
O(12)	6626(9)	3233(17)	-1093(16)
O(13)	6845(9)	1387(15)	144(16)
O(14)	6086(9)	3239(16)	810(14)
C(15)*	5411(26)	1809(46)	-997(47)
C(16)*	5320(47)	1059(87)	-298(90)
C(17)	5341(15)	1101(30)	-1161(28)
C(18)	5563(18)	764(33)	-1680(31)
C(19)*	5233(27)	679(50)	-429(43)
C(20)*	4872(27)	993(55)	-1500(47)
C(21)*	4999(32)	618(55)	-1124(57)
C(22)*	5059(31)	1884(55)	-1507(52)
C(23)	6539(13)	1199(24)	-145(22)
C(24)	6963(16)	1230(29)	-148(26)
C(25)	7007(15)	1937(27)	-2497(26)
C(26)	7245(14)	1143(27)	-1531(23)
C(27)	7022(19)	582(37)	-2636(34)
C(28)	5519(14)	3551(27)	-909(26)
C(29)	5520(16)	4350(29)	-877(28)
C(30)	5842(15)	4659(26)	-1261(27)
C(31)	5144(14)	4631(26)	-1239(24)
C(32)	5508(12)	4613(22)	-128(23)
C(33)	5839(11)	1154(21)	1105(21)
C(34)	5982(15)	1167(28)	1867(24)
C(35)	5755(17)	561(31)	2190(29)
C(36)	5276(13)	1891(23)	2199(22)
C(37)	6408(17)	1057(28)	1865(25)
C(38)	6496(11)	0(23)	-10(20)
C(39)	6314(12)	-693(21)	-140(21)
C(40)	6303(11)	-862(19)	-927(18)
C(41)	5902(13)	-734(24)	129(25)
C(42)	6595(11)	-1283(18)	216(21)
C(43)	5223(13)	2982(23)	916(22)

Table IX. Continued.

Atom	10^4 x	10^4 y	10^4 z
C(44)	4811(13)	2732(25)	1011(23)
C(45)	4637(15)	3134(28)	1581(26)
C(46)	4783(13)	1926(23)	1167(24)
C(47)	4640(13)	2808(25)	276(26)
C(48)	6122(12)	3062(21)	-2504(21)
C(49)	5884(13)	2986(23)	-3127(22)
C(50)	5956(14)	2280(28)	-3423(23)
C(51)	5456(16)	3080(28)	-2963(27)
C(52)	6046(20)	3489(40)	-3683(34)
C(53)	6973(13)	3435(26)	-953(24)
C(54)	7183(16)	4083(29)	-1247(27)
C(55)	6884(15)	4728(28)	-1282(27)
C(56)	7514(16)	4153(27)	-814(24)
C(57)	7263(16)	3813(31)	-2066(27)
C(58)	7125(15)	1852(25)	353(25)
C(59)	7450(15)	1440(26)	662(23)
C(60)	7763(21)	1983(27)	932(40)
C(61)	7374(16)	834(31)	1221(31)
C(62)	7672(19)	1160(35)	57(32)
C(63)	6444(17)	3511(30)	986(28)
C(64)	6457(18)	4139(29)	1582(27)
C(65)	6865(26)	4247(48)	1875(44)
C(66)	6076(22)	4419(42)	1720(38)
C(67)	6260(30)	3698(60)	2391(54)
Cl(68)	3606(12)	3455(22)	175(18)
Cl(69)	3207(14)	2726(27)	1479(24)

(a) Atoms marked by an asterisk were disordered. (b) The occupancy factor on the Cl atoms refined to an average value of 0.33.

Table X. Fractional Coordinates for the $\text{Mo}_3\text{O}(\text{O}-i\text{-Pr})_{10}$
Molecules.

Atom	10^4 x	10^4 y	10^4 z
Mo(1)	2300(1)	6934(1)	6254(1)
Mo(2)	3648(1)	7759(1)	6610(1)
Mo(3)	2788(1)	8263(1)	6608(1)
O(4)	7076(5)	2311(5)	2074(8)
O(5)	7097(5)	2384(4)	5092(8)
O(6)	6109(5)	1216(5)	3242(9)
O(7)	6910(5)	3322(4)	3861(9)
O(8)	8239(4)	2503(5)	3709(8)
O(9)	7375(5)	1227(4)	4670(8)
O(10)	8286(4)	3777(4)	5333(9)
O(11)	5658(5)	2145(5)	4631(9)
O(12)	5726(5)	2162(5)	1894(9)
O(13)	7269(5)	1140(5)	1905(9)
O(14)	8192(5)	3664(5)	2561(9)
C(15)	7071(7)	2409(7)	6517(13)
C(16)	7819(8)	2591(7)	7190(13)
C(17)	6482(8)	1713(8)	6760(15)
C(18)	5450(7)	566(7)	3365(16)
C(19)	5667(9)	26(8)	3670(17)
C(20)	4951(9)	321(9)	2037(16)
C(21)	6870(9)	3957(8)	4380(16)
C(22)	6772(10)	3959(9)	5882(16)
C(23)	6223(8)	3934(8)	3599(16)
C(24)	8962(7)	2565(8)	5808(14)
C(25)	-692(8)	2833(9)	5262(15)
C(26)	-604(8)	3073(8)	2921(15)
C(27)	2578(8)	-574(7)	5489(14)
C(28)	8140(8)	712(8)	4053(15)
C(29)	7385(10)	352(9)	5907(15)
C(30)	8957(7)	+407(7)	5470(14)
C(31)	-698(9)	4619(8)	6925(15)
C(32)	1155(8)	4986(7)	4951(15)
C(33)	4966(9)	2128(10)	4483(20)
C(34)	4395(11)	1481(16)	3876(24)
C(35)	4808(12)	2151(26)	5940(28)
C(36)	5806(8)	2182(7)	506(13)
C(37)	5533(8)	2688(9)	135(17)
C(38)	5353(8)	1418(8)	-285(14)
C(39)	7189(8)	1101(7)	467(13)
C(40)	3136(9)	-308(8)	10168(15)
C(41)	7911(9)	1538(8)	91(15)
C(42)	8081(7)	3612(7)	1143(13)
C(43)	7572(9)	3907(9)	839(16)

Table X. Continued.

Atom	10^4 x	10^4 y	10^4 z
C(44)	8814(9)	4024(8)	657(14)
Mo(1)	7204(1)	6927(1)	477(1)
Mo(2)	8128(1)	8165(1)	1681(1)
Mo(3)	8385(1)	7143(1)	1656(1)
O(4)	2415(4)	2724(4)	7515(8)
O(5)	1740(4)	2445(4)	53(8)
O(6)	971(4)	1809(4)	7494(8)
O(7)	2868(5)	2170(5)	-669(9)
O(8)	2410(4)	3770(4)	9442(8)
O(9)	863(5)	2990(5)	9145(8)
O(10)	3146(5)	3384(5)	1455(8)
O(11)	1378(5)	1025(4)	-834(8)
O(12)	1926(5)	1295(4)	6708(8)
O(13)	1490(5)	3222(5)	6816(8)
O(14)	3725(5)	3660(5)	9085(9)
C(15)	1431(6)	2367(6)	1302(11)
C(16)	1812(7)	2100(7)	2217(13)
C(17)	616(7)	1856(7)	1003(14)
C(18)	322(7)	1297(7)	6652(12)
C(19)	242(7)	1585(7)	5385(12)
C(20)	314(7)	-1140(7)	2557(13)
C(21)	3385(7)	1941(7)	-336(13)
C(22)	2194(8)	1608(8)	874(14)
C(23)	3383(8)	1435(8)	847(14)
C(24)	2494(7)	4459(6)	1074(13)
C(25)	2151(8)	4415(8)	1286(13)
C(26)	3300(8)	5014(7)	10209(14)
C(27)	347(7)	3139(7)	8525(12)
C(28)	655(7)	3929(7)	8494(14)
C(29)	-302(7)	287(8)	-733(15)
C(30)	3841(8)	3051(8)	2105(13)
C(31)	3758(9)	4271(9)	3457(15)
C(32)	4301(10)	3552(10)	2406(21)
C(33)	8720(7)	-324(6)	1173(13)
C(34)	635(7)	-117(7)	7722(13)
C(35)	8876(8)	9986(7)	9905(13)
C(36)	1980(7)	1455(6)	5398(11)
C(37)	2770(7)	1752(6)	5138(13)
C(38)	8525(8)	-764(7)	5606(13)
C(39)	1933(7)	3447(7)	5782(13)
C(40)	1449(8)	3390(8)	4566(13)
C(41)	2515(8)	4212(7)	6303(13)
C(42)	4056(9)	3615(10)	7927(19)
C(43)	4782(14)	3707(17)	-1614(33)
C(44)	4190(18)	4170(26)	7281(36)

Table XI. Bond Distances (\AA) for the $\text{Mo}_3\text{O}(\text{OR})_{10}$ Molecules.

Bond	Distance R = i-Pr		Distance R = CH_2 -t-Bu
	I	II	
Mo(1)-Mo(2)	2.538(2)	2.534(2)	2.523(5)
Mo(1)-Mo(3)	2.535(2)	2.528(2)	2.524(6)
Mo(2)-Mo(3)	2.539(2)	2.528(2)	2.539(5)
avg. [Mo-Mo]	2.534		2.529
Mo(1)-O(4)	2.064(8)	2.055(7)	2.036(25)
Mo(2)-O(4)	2.064(8)	2.058(8)	2.039(24)
Mo(3)-O(4)	2.068(8)	2.059(8)	2.026(30)
avg. [Mo-(μ_3 -O)]	2.061		2.034
Mo(1)-O(5)	2.173(8)	2.155(7)	2.153(32)
Mo(2)-O(5)	2.172(8)	2.157(7)	2.245(32)
Mo(3)-O(5)	2.165(7)	2.139(7)	2.238(33)
avg. [Mo-(μ_3 -OR)]	2.160		2.212
Mo(1)-O(7)	2.015(8)	2.023(8)	2.025(28)
Mo(1)-O(8)	2.036(7)	2.054(7)	2.024(30)
Mo(2)-O(6)	2.024(8)	2.024(7)	2.026(26)
Mo(2)-O(7)	2.043(8)	2.041(8)	1.965(28)
Mo(3)-O(6)	2.053(9)	2.047(7)	2.027(24)
Mo(3)-O(8)	2.009(8)	2.014(7)	2.040(28)
avg. [Mo-(μ_2 -OR)]	2.032		2.018
Mo(1)-O(14)	1.891(8)	1.907(8)	1.842(30)
Mo(2)-O(12)	1.910(8)	1.912(7)	1.868(32)
Mo(3)-O(13)	1.893(8)	1.912(8)	1.857(31)
avg. [Mo-OR]	1.904		1.856
Mo(1)-O(10)	1.952(7)	1.959(8)	1.930(25)
Mo(2)-O(11)	1.953(8)	1.945(8)	1.936(23)
Mo(3)-O(9)	1.950(8)	1.950(8)	1.960(26)
avg. [Mo-OR]	1.952		1.942

Table XII. Bond Angles for the $\text{Mo}_3\text{O}(\text{OR})_{10}$ Molecules.

Bond	Angle R = i-Pr		Angle R = CH_2 -t-Bu
	I	II	
Mo(2)-Mo(1)-Mo(3)	60.1(1)	59.9(1)	60.4(2)
Mo(2)-Mo(1)-O(4)	52.1(2)	52.0(2)	51.8(7)
Mo(2)-Mo(1)-O(5)	54.2(2)	54.1(2)	56.7(9)
Mo(2)-Mo(1)-O(7)	51.8(2)	51.7(2)	49.7(8)
Mo(2)-Mo(1)-O(8)	110.8(2)	110.7(2)	111.9(8)
Mo(2)-Mo(1)-O(10)	127.7(2)	126.8(3)	128.3(7)
Mo(2)-Mo(1)-O(14)	123.9(2)	127.9(3)	120.5(9)
Mo(3)-Mo(1)-O(4)	52.2(2)	52.2(2)	51.4(8)
Mo(3)-Mo(1)-O(5)	54.1(2)	53.7(2)	56.5(9)
Mo(3)-Mo(1)-O(7)	111.6(2)	111.6(2)	109.9(8)
Mo(3)-Mo(1)-O(8)	50.7(2)	50.9(2)	51.9(8)
Mo(3)-Mo(1)-O(10)	127.6(2)	127.7(2)	128.3(9)
Mo(3)-Mo(1)-O(14)	126.8(2)	125.6(3)	123.6(9)
O(4)-Mo(1)-O(5)	92.3(3)	91.9(3)	94.5(11)
O(4)-Mo(1)-O(7)	87.3(3)	83.6(3)	86.3(11)
O(4)-Mo(1)-O(8)	83.9(3)	85.5(3)	88.2(12)
O(4)-Mo(1)-O(10)	179.7(3)	178.8(3)	179.7(12)
O(4)-Mo(1)-O(14)	87.1(3)	88.8(3)	83.9(13)
O(5)-Mo(1)-O(7)	81.1(3)	85.1(3)	80.0(10)
O(5)-Mo(1)-O(8)	83.3(3)	81.4(3)	79.8(11)
O(5)-Mo(1)-O(10)	87.4(3)	87.2(3)	85.4(12)
O(5)-Mo(1)-O(14)	177.7(3)	177.8(3)	177.1(12)
O(7)-Mo(1)-O(8)	161.7(3)	162.4(3)	158.5(11)
O(7)-Mo(1)-O(10)	92.6(3)	95.5(3)	94.0(12)
O(7)-Mo(1)-O(14)	96.7(3)	97.1(3)	97.5(11)
O(8)-Mo(1)-O(10)	96.1(3)	95.3(3)	91.5(13)
O(8)-Mo(1)-O(14)	98.8(3)	96.5(3)	102.5(11)
O(10)-Mo(1)-O(14)	93.3(3)	92.5(3)	96.2(13)
Mo(1)-Mo(2)-Mo(3)	59.9(1)	59.9(1)	59.8(2)
Mo(1)-Mo(2)-O(4)	52.1(2)	51.9(2)	51.7(7)
Mo(1)-Mo(2)-O(5)	54.3(2)	54.0(2)	53.3(8)
Mo(1)-Mo(2)-O(6)	111.8(2)	111.9(2)	110.3(7)
Mo(1)-Mo(2)-O(7)	50.8(2)	51.1(2)	51.8(8)
Mo(1)-Mo(2)-O(11)	128.9(2)	125.4(2)	129.1(8)
Mo(1)-Mo(2)-O(12)	123.2(3)	127.9(2)	123.8(10)
Mo(3)-Mo(2)-O(4)	52.1(2)	52.1(2)	51.1(8)
Mo(3)-Mo(2)-O(5)	54.0(2)	53.6(2)	55.4(8)
Mo(3)-Mo(2)-O(6)	52.0(2)	52.0(2)	51.2(7)
Mo(3)-Mo(2)-O(7)	110.5(2)	111.0(2)	111.4(8)
Mo(3)-Mo(2)-O(11)	126.9(3)	126.9(2)	129.1(10)
Mo(3)-Mo(2)-O(12)	126.9(3)	123.2(2)	121.9(10)
O(4)-Mo(2)-O(5)	92.3(3)	91.8(3)	91.7(12)
O(4)-Mo(2)-O(6)	86.5(3)	85.2(3)	88.9(11)
O(4)-Mo(2)-O(7)	86.5(3)	83.1(3)	87.8(11)
O(4)-Mo(2)-O(11)	178.5(3)	177.3(3)	179.2(11)

Table XII. Continued.

Bond	Angle R = i-Pr		Angle R = CH ₂ -t-Bu
	I	II	
O(4)-Mo(2)-O(12)	86.7(3)	87.4(3)	84.8(13)
O(5)-Mo(2)-O(6)	82.0(3)	83.5(3)	79.0(11)
O(5)-Mo(2)-O(7)	80.5(3)	84.7(3)	79.1(10)
O(5)-Mo(2)-O(11)	87.7(3)	85.9(3)	89.0(12)
O(5)-Mo(2)-O(12)	177.0(3)	175.8(3)	176.5(13)
O(6)-Mo(2)-O(7)	160.9(3)	163.0(3)	157.7(11)
O(6)-Mo(2)-O(11)	92.0(3)	95.9(3)	90.8(12)
O(6)-Mo(2)-O(12)	100.7(3)	92.3(3)	101.1(12)
O(7)-Mo(2)-O(11)	94.9(3)	95.4(3)	92.7(12)
O(7)-Mo(2)-O(12)	96.7(3)	99.3(3)	100.6(13)
O(11)-Mo(2)-O(12)	93.4(3)	95.0(3)	94.5(13)
Mo(1)-Mo(3)-Mo(2)	60.0(0)	60.2(0)	59.8(1)
Mo(1)-Mo(3)-O(4)	52.1(2)	52.0(2)	51.8(7)
Mo(1)-Mo(3)-O(5)	54.4(2)	54.2(2)	53.3(8)
Mo(1)-Mo(3)-O(6)	110.9(2)	111.4(2)	110.2(8)
Mo(1)-Mo(3)-O(8)	51.7(2)	52.3(2)	51.3(9)
Mo(1)-Mo(3)-O(9)	125.9(2)	127.6(2)	129.4(8)
Mo(1)-Mo(3)-O(13)	127.3(3)	126.3(2)	125.2(10)
Mo(2)-Mo(3)-O(4)	52.0(2)	52.1(2)	51.6(7)
Mo(2)-Mo(3)-O(5)	54.3(2)	54.3(2)	55.6(8)
Mo(2)-Mo(3)-O(6)	51.0(2)	51.2(2)	51.2(7)
Mo(2)-Mo(3)-O(8)	111.7(2)	112.4(2)	110.7(9)
Mo(2)-Mo(3)-O(9)	128.6(2)	128.0(2)	133.1(8)
Mo(2)-Mo(3)-O(13)	124.7(3)	125.9(2)	125.0(9)
C(4)-Mo(3)-O(5)	92.4(3)	92.3(2)	92.2(10)
O(4)-Mo(3)-O(6)	85.7(3)	84.6(3)	89.2(10)
O(4)-Mo(3)-O(8)	84.4(3)	86.4(3)	88.0(11)
O(4)-Mo(3)-O(9)	177.7(3)	179.0(3)	175.3(11)
O(4)-Mo(3)-O(13)	88.0(3)	88.2(3)	85.9(12)
O(5)-Mo(3)-O(6)	81.5(3)	83.4(3)	79.1(11)
O(5)-Mo(3)-O(8)	84.2(3)	82.8(3)	77.5(12)
O(5)-Mo(3)-O(9)	86.7(3)	87.5(3)	91.6(11)
O(5)-Mo(3)-O(13)	177.7(4)	179.5(3)	178.2(13)
O(6)-Mo(3)-O(8)	162.2(3)	163.2(3)	156.3(11)
O(6)-Mo(3)-O(9)	96.2(3)	95.7(3)	94.2(11)
O(6)-Mo(3)-O(13)	96.3(4)	96.3(3)	100.9(12)
O(8)-Mo(3)-O(9)	93.4(3)	93.2(3)	90.1(12)
O(8)-Mo(3)-O(13)	98.1(3)	97.6(3)	102.4(13)
O(9)-Mo(3)-O(13)	92.9(3)	92.0(3)	90.2(13)
Mo(1)-O(4)-Mo(2)	75.9(3)	76.1(3)	76.5(9)
Mo(1)-O(4)-Mo(3)	75.7(3)	75.8(3)	76.8(10)
Mo(2)-O(4)-Mo(3)	75.8(3)	75.7(3)	77.3(10)
Mo(1)-O(5)-Mo(2)	71.5(2)	72.0(2)	70.0(10)
Mo(1)-O(5)-Mo(3)	71.5(2)	72.1(2)	70.2(10)

Table XII. Continued.

Bond	Angle R = i-Pr		Angle R = CH ₂ -t-Bu
	I	II	
Mo(2)-O(6)-Mo(3)	77.1(3)	76.8(3)	77.6(9)
Mo(1)-O(7)-Mo(2)	77.4(3)	77.2(3)	78.4(10)
Mo(1)-O(8)-Mo(3)	77.6(3)	76.8(3)	76.8(10)
Mo-O-C α in alkoxide	129.0(10) average		129.0(10) average
O-C α -C β in alkoxide	108.9(11) average		112.0(40) average
C β -C α -C β in alkoxide	110.8(13) average		109.0(51) average

Table XIII. Fractional Coordinates for the $\text{Mo}_6\text{O}_{10}(\text{O}-i\text{-Pr})_{12}$

Molecule.

Atom	$10^4 x$	$10^4 y$	$10^4 z$
Mo(1)	1285.4(2)	104.2(3)	-124.9(3)
Mo(2)	2776.6(2)	-1044.0(3)	-1053.6(3)
Mo(3)	2878.3(2)	-3886.8(3)	-2919.9(3)
O(4)	1897(2)	1560(2)	656(2)
O(5)	3811(2)	102(2)	-527(3)
O(6)	2425(2)	-4552(2)	-4658(3)
O(7)	1723(2)	9518(2)	7983(2)
O(8)	1935(2)	-1041(2)	546(2)
O(9)	-88(2)	191(2)	-1148(2)
O(10)	3086(2)	-2044(2)	-3053(2)
O(11)	3323(2)	-2541(2)	-797(2)
O(12)	1582(2)	-3505(2)	-2230(3)
O(13)	2821(2)	-5233(2)	-2193(3)
C(14)	4301(2)	-3763(2)	-3129(3)
C(15)	-160(3)	424(4)	-2556(4)
C(16)	-13(4)	1782(5)	-2328(5)
C(17)	-1117(4)	-345(4)	-3459(5)
C(18)	3121(3)	-1741(3)	-4410(4)
C(19)	2043(3)	-2031(4)	-5174(4)
C(20)	3629(3)	9592(4)	5860(5)
C(21)	3510(3)	-2893(3)	495(4)
C(22)	2519(3)	-3539(4)	945(4)
C(23)	4065(3)	-1766(4)	1671(4)
C(24)	547(3)	-4068(4)	2897(4)
C(25)	9870(4)	6875(5)	7355(9)
C(26)	152(5)	-5113(6)	-2327(10)
C(27)	3328(3)	-6280(4)	-2573(5)
C(28)	2669(4)	-7252(4)	-3843(5)
C(29)	3445(4)	-6778(5)	-1270(6)
C(30)	5313(3)	3166(4)	-2432(4)
C(31)	5664(3)	-1997(4)	-2848(6)
C(32)	6040(4)	-4076(5)	-2843(6)

Table XIV. Selected Bond Distances (Å) for the Centrosymmetric $\text{Mo}_6\text{O}_{10}(\text{O}-i\text{-Pr})_{12}$ Molecule.

Bond	Distance (Å)	Bond	Distance (Å)
Mo(1)-Mo(2)	2.585(1)	Mo(3)-O(6)	1.691(2)
Mo(1)-O(4)	1.675(2)	Mo(3)-O(10)	2.128(2)
Mo(1)-O(7)	1.921(2)	Mo(3)-O(11)	2.197(2)
Mo(1)-O(8)	1.926(2)	Mo(3)-O(12)	1.919(2)
Mo(1)-O(9)	2.058(2)	Mo(3)-O(13)	1.806(2)
Mo(2)-O(5)	1.671(2)	Mo(3)-O(14)	1.865(2)
Mo(2)-O(7)	1.939(2)	Mo(2)-Mo(3)	3.285(1)
Mo(2)-O(8)	1.939(2)	Mo(1)-Mo(1)'	3.353(1)
Mo(2)-O(10)	2.057(2)	O-Ca in iso-propoxide	1.45(1) average
Mo(2)-O(11)	2.044(2)	Ca-Cβ in iso-propoxide	1.51(1) average
Mo(2)-O(12)	2.880(2)	C-H in iso-propoxide	0.97(5) average

Table XV. Selected Bond Angles for the Centrosymmetric $\text{Mo}_6\text{O}_{10}(\text{O}-i\text{-Pr})_{12}$ Molecule.

Bond	Angle ($^\circ$)	Bond	Angle ($^\circ$)
Mo(2)-Mo(1)-O(4)	103.7(1)	O(10)-Mo(2)-O(11)	73.3(1)
Mo(2)-Mo(1)-O(7)	48.5(1)	O(6)-Mo(3)-O(10)	94.9(1)
Mo(2)-Mo(1)-O(8)	48.2(1)	O(6)-Mo(3)-O(11)	162.8(1)
Mo(2)-Mo(1)-O(9)	131.2(1)	O(6)-Mo(3)-O(12)	96.6(1)
O(4)-Mo(1)-O(7)	109.9(1)	O(6)-Mo(3)-O(13)	103.2(1)
O(4)-Mo(1)-O(8)	110.8(1)	O(6)-Mo(3)-O(14)	98.9(1)
O(4)-Mo(1)-O(9)	104.8(1)	O(10)-Mo(3)-O(11)	68.9(1)
O(7)-Mo(1)-O(8)	92.1(1)	O(10)-Mo(3)-O(12)	82.0(1)
O(7)-Mo(1)-O(9)	142.7(1)	O(10)-Mo(3)-O(13)	161.8(1)
O(8)-Mo(1)-O(9)	140.3(1)	O(10)-Mo(3)-O(14)	85.8(1)
O(9)-Mo(1)-O(9)	71.5(1)	O(11)-Mo(3)-O(12)	75.7(1)
Mo(1)-Mo(2)-O(5)	101.3(1)	O(11)-Mo(3)-O(13)	92.8(1)
Mo(1)-Mo(2)-O(7)	47.7(1)	O(11)-Mo(3)-O(14)	86.4(1)
Mo(1)-Mo(2)-O(8)	47.8(1)	O(12)-Mo(3)-O(13)	94.3(1)
Mo(1)-Mo(2)-O(10)	133.5(1)	O(12)-Mo(3)-O(14)	161.1(1)
Mo(1)-Mo(2)-O(11)	136.3(1)	O(13)-Mo(3)-O(14)	92.9(1)
O(5)-Mo(2)-O(7)	102.4(1)	Mo(1)-O(7)-Mo(2)	84.1(1)
O(5)-Mo(2)-O(8)	109.2(1)	Mo(1)-O(8)-Mo(2)	83.9(1)
O(5)-Mo(2)-O(10)	105.8(1)	Mo(1)-O(9)-Mo(1)	108.5(1)
O(5)-Mo(2)-O(11)	103.5(1)	Mo(2)-O(10)-Mo(3)	103.4(1)
O(7)-Mo(2)-O(8)	91.1(1)	Mo(1)-Mo(2)-Mo(3)	134.3(1)
O(7)-Mo(2)-O(10)	87.1(1)	Mo(1)-Mo(1)-Mo(2)	146.5(1)
O(7)-Mo(2)-O(11)	145.8(1)	Mo-O-Ca in iso-propoxide	130.0(10) average
O(8)-Mo(2)-O(10)	145.7(1)	Ca-Ca-Ca in iso-propoxide	113.0(10) average
O(8)-Mo(2)-O(11)	89.9(1)	O-Ca-Ca in isopropoxide	109.0(10) average

Table XVII. Summary of Crystallographic Data.

	I	II	III	IV
fw	448.37	1260.17	894.70	1444.69
space group	$P\bar{1}$	Pbcn	$P\bar{1}$	$P\bar{1}$
a, A	13.907(6)	35.557(19)	21.274(6)	13.082(3)
b, A	8.413(3)	18.969(9)	21.808(5)	11.478(2)
c, A	19.999(8)	19.342(9)	10.207(2)	9.760(2)
alpha, deg	111.02(1)		98.69(1)	106.40(1)
beta, deg	71.37(2)		92.92(1)	91.85(1)
gamma, deg	88.98(1)		118.03(1)	99.81(1)
Z	4	8	4	1
V, A ³	2046.39	13045.59	4091.77	1380.34
density(calcd), g/cm ³	1.455	1.283	1.452	1.738
crystal dimensions, mm	.13 .14 .12	.12 .14 .16	.08 .16 .25	.22 .21 .26
crystal color	brownish	green	green	orange
radiation		Mo K α ($\lambda=0.71069$ A) graphite monochromator		
linear abs coeff, cm ⁻¹	6.49	6.83	9.30	13.57
temp, deg C	-161	-161	-162	-162

Table XVII. Continued.

	I	II	III	IV
instrument		Picker 4-circle diffractometer locally modified and interfaced		
detector aperture		3.0 mm wide x 4.0 mm high 22.5 cm from crystal		
sample to source distance		23.5 cm		
takeoff angle, deg	2.0	2.0	2.0	2.0
scan speed, deg/min	3.5	2.5	3.0	5.0
scan width, deg	1.7	1.0	2.0	2.0
	all plus dispersion correction of $0.692 \tan \theta$			
bkgd counts, = at each end of scan	3	3	4	3
2 theta range, deg	6 - 45	6 - 40	6 - 40	6 - 50
data collected	5694	10379	11676	5643
unique data	5353	6102	10717	4891
unique data with $F_o > 3\sigma(F_o)$	4021	2830	7711	4388
no. of variables	469	293	793	457
R(F)	0.067	0.075	0.070	0.027
Rw(F)	0.068	0.076	0.066	0.036
goodness of fit	1.494	1.558	1.358	1.171
largest delta/sigma	0.05	0.04	0.05	0.03

I = $\text{MoO}_2(\text{O-i-Pr})_2(\text{opy}) \cdot \frac{1}{2} \text{toluene}$

II = $\text{Mo}_3\text{O}(\text{OCH}_2\text{-t-Bu})_{10} \cdot \frac{1}{3} \text{CH}_2\text{Cl}_2$

III = $\text{Mo}_3\text{O}(\text{O-i-Pr})_{10}$

IV = $\text{Mo}_6\text{O}_{10}(\text{O-i-Pr})_{12}$

Some
 Table XVI. Structural Properties for Diamagnetic Compounds Containing a Central $\text{Mo}_2\text{O}_4^{2+}$ Moiety.

Compound	d(M-M) Å	d(Mo-O) Å terminal	d(Mo-O) Å bridge	Magnetic property	Reference
$\text{Mo}_6\text{O}_{10}(\text{O-i-P})_{12}$	2.585(1)	1.67(1)	1.93(1)	diamagnetic	this work
$\text{Mo}_4\text{O}_8(\text{O-i-Pr})_2(\text{py})_4$	2.600(1)	1.68(1), 1.70(1)	1.94(1)	diamagnetic	39
$\text{Mo}_2\text{O}_4(\text{C}_2\text{O}_4)_2(\text{H}_2\text{O})_2^{2-}$	2.541(2)	1.70(3)	1.91(3)	diamagnetic	54
$\text{Mo}_2\text{O}_4(\text{cys})_2^{2-}$	2.569(2)	1.71(2)	1.93(2)	diamagnetic	55
$\text{Mo}_2\text{O}_4(\text{Etcys})_2$	2.569(2)	1.71(2)	1.93(2)	diamagnetic	56